

Interplay of quantum statistics and self-interference in extended colliders

Sai Satyam Samal,¹ Smitha Vishveshwara,² Yuval Gefen,³ and Jukka I. Väyrynen¹

¹*Department of Physics and Astronomy, Purdue University, West Lafayette, Indiana 47907, USA*

²*Department of Physics, University of Illinois Urbana-Champaign, Urbana, Illinois 61801, USA*

³*Department of Condensed Matter Physics, The Weizmann Institute of Science, Rehovot 76100, Israel*

(Dated: December 30, 2024)

Collision of quantum particles remains an effective way of probing their mutual statistics. Colliders based on quantum point contacts in quantum Hall edge states have been successfully used to probe the statistics of the underlying quantum particles. Notwithstanding the extensive theoretical work focusing on point-like colliders, when it comes to experiment, the colliders are rarely point-like objects and can support a resonant level or multiple tunneling points. We present a study of a paradigmatic extended (non-point-like) fermionic collider which is readily generalized to colliding bosons. As with particle interferometers, in an extended collider there is an infinite number of trajectories for any single or multi-particle event. Self-interference of the former can lead to an apparent bunching of fermions when we compare the cross-current correlator with the classical benchmark representing two active sources. In view of this apparent bunching behavior of fermions, we identify an irreducible cross-current correlator which reveals the true mutual statistics of fermions.

Introduction.— Braiding statistics constitutes a fundamental property of quantum particles and encodes how the wave function changes under the adiabatic encircling of one particle by another [1]. Two-dimensional platforms, e.g. 2D electron gas (2DEG) setups, may accommodate anyons, whose fractional statistics is intermediate between fermions and bosons [1–5]. Fractional quantum Hall phases provide canonical platforms with a promise to observe and manipulate such exotic quasi-particles [6–8]. Concurrent with interference-based theoretical proposals [9–14] and their subsequent experimental realization [15–26], complementary and arguably simpler methods avoiding the use of interference have been developed to probe quantum statistics. The latter method is based on so-called “colliders” where incoming quantum particles experience statistical interaction and are then detected by measuring electrical currents. Cross-current correlations [27] in Hanbury-Brown and Twiss settings that employ quantum Hall edge states [28–35] have been shown to contain information of the underlying statistics.

With point-like colliders, the statistics of quantum particles is determined by measuring current auto-correlations or cross-correlations [27, 35–42]. To determine the emergence of excess or deficiency of particle bunching, one needs to compare these correlations to a benchmark [33–37, 43]. There are two candidate benchmarks which produce identical results in the case of a point-like collider. One is the corresponding cross-current correlator resulting from the collision of non-interacting, distinguishable classical particles [27, 43]. The second is the reducible part of the cross-current correlator [44] which incorporates all the single-particle contributions to the cross-current correlations (including interference effects). Interestingly, the latter benchmark is equivalent to the cross-current correlator associated with classical waves. Following this guiding principle, Laugh-

lin anyons have been shown to give rise to boson-like bunching, quantitatively intermediate between bosons and classical particles [28–35, 38–41].

The interpretation of recent experiments [38–41] draws on advances in the theory of point-like colliders [35–37]. Notably, realistic experimental platforms may have resonant levels, caused for instance by multiple tunneling bridges in the collider area. (Resonances are routinely observed in the quantum point contact transmission curve, see e.g. Ref. [39].) In such an “extended collider”, multiple trajectories can connect the source and the drain, and interference effects may distort the statics-based results.

Generalizing to non-point-like colliders, we show here that the above two benchmarks lead to different results. This implies that the choice of a correct benchmark is crucial. We find that employing the first benchmark to determine the boson-like or fermion-like nature of the particle-statistics is fundamentally flawed. One may obtain an *apparent* statistical transmutation [43], i.e. fermions that seemingly tend to bunch. The origin of this observation relates to each particle’s self-interference contributions, having nothing to do with quantum statistics. Employing the second benchmark, i.e., subtracting the reducible part from the cross-current correlator, one removes single-particle self-interference contributions, leading to a genuine quantum statistics witness. Thus, the second benchmark correctly captures the statistics of the colliding particles. In a point-like collider, single-particle self-interference terms are absent, which is why the two benchmarks lead to identical results.

Technically, the presence of self-interference can be identified by evaluating a time-resolved current correlator, which is proportional to the density-density correlation function $g^{(2)}$ [45] [see Eq. (6)]. This function represents an efficient tool to distinguish a point-like collider from the extended one. Additionally, we show that $g^{(2)}$ (with the appropriate benchmark subtracted) is also sen-

sitive to the mutual statistics and hence can distinguish fermions and bosons.

Our analysis here employs a fermionic collider (we also give results for bosonic colliders where applicable). We note that focusing on such fundamental platforms offers two advantages: First, antibunching (bunching) of fermions (bosons) is more extreme than that of intermediate statistics of anyons. Demonstrating false statistical transmutation in that case is thus more striking. Second, we can avoid the complication due to topological vacuum-bubbles braiding [37], also known as time-domain braiding [35, 36, 46], thus facilitating a clear message concerning false bunching of fermions.

Below, we first introduce a simple model of an extended collider that captures the relevant physics. We then consider a two-particle collision, demonstrating that the incorrect benchmark leads to apparent fermion bunching, leading us to identify the role of self-interference and define the proper statistical benchmark. Finally, we demonstrate that the results of our analysis can be tested in experiments by measuring dc (zero frequency) auto- and cross-current correlators. Additional information, such as the spatial size of the extended collider, can be obtained from time-resolved correlators, such as the $g^{(2)}$ -function.

Model and qualitative description of apparent bunching.— Our model consists of two one-dimensional chiral channels emanating from sources S_1 and S_2 , and terminating at the respective drains D_1 and D_2 , where particles can be detected (e.g., by measuring currents). These channels are tunnel-coupled to the extended collider. The latter is modelled by a quantum anti-dot (QAD) encircled by a single chiral channel, cf. Fig. 1a. Arriving at the collider, particles (wave packets) from the source (S_1 or S_2) can tunnel to and wind around the QAD an arbitrary number of times, before escaping to a detector drain (D_1 or D_2). The S -matrix at each channel-QAD junction (represented by a dashed line in Fig. 1a), is given by ($r > 0$),

$$S = \begin{pmatrix} \rho_1 & \tau_1 \\ \tau_2 & \rho_2 \end{pmatrix} = \begin{pmatrix} re^{i\theta} & i\sqrt{1-r^2} \\ i\sqrt{1-r^2} & re^{-i\theta} \end{pmatrix}. \quad (1)$$

For simplicity we assume time reversal symmetry for each edge-QAD scatterer, see Sec. II B of SM [47] for non-identical case.

The origin of apparent fermion bunching in the extended collider setup can be simply understood by considering the limit of a small edge-collider tunneling amplitude, $t = \sqrt{1-r^2} \ll 1$, and calculating the probability of a two-particle “anti-bunching event”, $P(11)_F$, Sec. III of SM [47]: the two colliding fermions end up each at a different drain. Here, apparent bunching-like behaviour corresponds to the inequality, $\mathcal{Q}_{Cl;F} = P(11)_F - P(11)_{Cl} \leq 0$, where comparison is with the corresponding benchmark $\mathcal{B}_1 = P(11)_{Cl}$ for classical par-

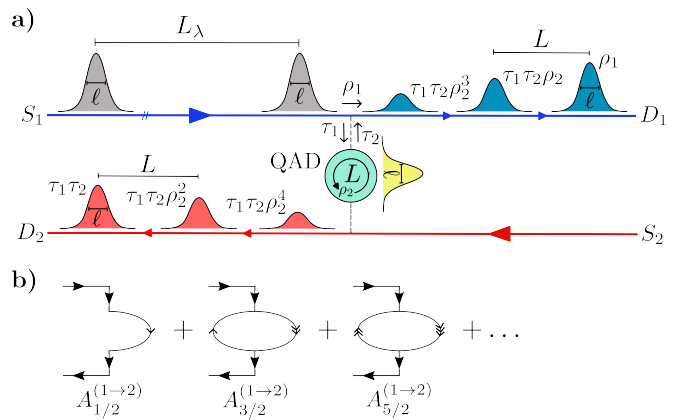


Figure 1. (a) Extended collider comprising two sources (S_1 , S_2) and two detectors (D_1 , D_2). A dilute beam having large separation L_λ between wave packets of width ℓ , emitted from S_1 , can give rise to a quasi-bound state at the collision area, a chiral quantum anti-dot (QAD) of circumference L . An incoming beam can tunnel into the QAD. As a result the outgoing beam comprises infinitely many wavelets of ever decreasing amplitude [determined by the junction tunneling amplitudes, Eq. (1)], spatially separated by L . (b) Processes that contribute to the amplitude to tunnel from S_1 to D_2 . The arrows in each segment of the QAD represent the number of times this segment was visited before being emitted from the QAD in the direction of D_2 . The processes involve half-integer number of windings, depicted by the subscript in the amplitude $A_{n+\frac{1}{2}}^{(1 \rightarrow 2)}$. Summing up these partial amplitudes facilitates evaluation of the “anti-bunching probability” $P(11)_{F/B}$ for fermions/bosons, Sec. III of SM, Ref. [47].

ticles. The latter probability, associated with two independent scattering events of classical particles, is equal to the sum of the probabilities of each of the contributing processes with no interference between different trajectories (or histories) [48]. For example, the event (to be denoted $1 \rightarrow 2$) where a particle goes from S_1 to D_2 , involves a particle transmitted through QAD, see Fig. 1b. The probability for this process is the sum of the squares of each amplitude in Fig. 1b, forming a geometric series $\mathcal{P}(1 \rightarrow 2)_{Cl} = t^4(1 + r^4 + \dots) = \frac{t^2}{2-t^2} \approx \frac{t^2}{2}$, for $t \ll 1$ [47]. Using conservation of probability, we get, $\mathcal{P}(1 \rightarrow 1)_{Cl} = 1 - \frac{t^2}{2}$. Hence, for two uncorrelated and non-interacting classical particles one then obtains $P(11)_{Cl} = \mathcal{P}(1 \rightarrow 1)_{Cl}^2 + \mathcal{P}(1 \rightarrow 2)_{Cl}^2 = 1 - t^2$.

Next, to obtain $P(11)_F$, we consider the leading quantum interference correction to the above result. In the leading approximation, we restrict ourselves to consider interference only between trajectories whose winding number differ at most by 1. Such partial interference is relevant for the case where the spatial width ℓ of the wave packets is smaller than the size L of the QAD, Fig. 1a. The ratio $\frac{\ell}{L}$ determines the degree of interference in the system. The limit $\frac{\ell}{L} \rightarrow 0$ produces the results for the classical particles (separate, non-overlapping

wave packets do not interfere) [48]. In the opposite limit $\frac{\ell}{L} \gg 1$, all trajectories interfere with each other.

For quantum particles, the correction due to self-interference of the single particle trajectories, Fig. 1b, modifies the single-particle tunneling probability to $\mathcal{P}(1 \rightarrow 2)_F = \frac{t^2}{2}(1 + 2c_1 \cos 2\alpha)$, where $c_1 \ll 1$ is a positive interference suppression factor ($c_1 = 0$ in the fully classical case) and $2\alpha = kL - 2\theta$ is the accumulated orbital phase [47]. With the above result, we find $P(11)_F \approx \mathcal{P}(1 \rightarrow 1)_F^2 = 1 - t^2(1 + 2c_1 \cos 2\alpha)$, showing apparent bunching of fermions, $\mathcal{Q}_{\text{Cl};F} = P(11)_F - P(11)_{\text{Cl}} = -2t^2 c_1 \cos 2\alpha \leq 0$ whenever $\cos 2\alpha \geq 0$. The bunching is largest near resonant tunneling [49], where the interference enhancement is maximized, $2\alpha/\pi = 0 \pmod{2}$. We note that this t^2 -correction to $P(11)_F$ is independent of statistics and thus the same result also holds for bosonic wave packets. The difference between bosons and fermions shows up in the interference phase between exchange ($1 \rightarrow 2$) and direct ($1 \rightarrow 1$) trajectories of the particles in order t^4 of the tunneling amplitude [47].

Partial interference in an extended collider.— Above, we demonstrated the apparent bunching of fermions ($\mathcal{Q}_{\text{Cl};F} \leq 0$) in the weak tunneling limit ($t \ll 1$) and with suppressed interference. Next, we present the evaluation of $P(11)_{F/B}$ in the generic case, for both fermions (F) and bosons (B). We start by discussing the single-particle processes, where self-interference plays an important role in an extended collider. Let $A_n^{(1 \rightarrow 1)}$ denote the single-particle amplitude of the process where the particle starts from S_1 and performs n windings before reaching D_1 . If we had full interference between different trajectories, the transmission probability would be $\mathcal{P}(1 \rightarrow 1)_{F/B} = |\sum_{n=0}^{\infty} A_n^{(1 \rightarrow 1)}|^2$, for both fermions and bosons, since we consider only a single particle. With partial interference (due to wave packet size or decoherence [50]), trajectories with large winding number mismatch interfere less. The probability $\mathcal{P}(1 \rightarrow 1)_{F/B}$ with partial interference can be obtained by the substitution, $A_n^{(1 \rightarrow 1)*} A_m^{(1 \rightarrow 1)} \rightarrow f(|n - m|) A_n^{(1 \rightarrow 1)*} A_m^{(1 \rightarrow 1)}$ where $f(|n - m|)$ is an appropriate decay function that depends on the wave packet shape, Sec. IV of SM [47]. The probability in the case of classical particles corresponds to the case with no interference ($f(|n - m|) = \delta_{m,n}$) and hence is equal to sum of the probabilities $\mathcal{P}(1 \rightarrow 1)_{\text{Cl}} = \sum_{n=0}^{\infty} |A_n^{(1 \rightarrow 1)}|^2$.

In practice, the sources emit wave packets with finite width which the extended collider breaks into a sequence of smaller wavelets, as depicted in Fig. 1a, giving rise to partial interference [47]. (For simplicity, we set $\hbar = 1$ and assume a linear dispersion relation so that the wave packets retain their shape and velocity.) With a scatterer of size L (see Fig. 1a), the particle with momentum k gains an orbital phase $\varphi = kL$. A single incoming wave packet starting from $(x_1^{(0)}, t_1^{(0)})$ in S_1 , after being transmitted to (x_1, t_1) in D_1 , is given as a convolution of the incoming

wave packet $\tilde{\phi}_{s_1}$ and the transmission function,

$$\tilde{\phi}_{d_1}(X) = \int_{-\infty}^{\infty} dx \tilde{\phi}_{s_1}(x - x_1^{(0)} + vt_1^{(0)}) \mathcal{T}(x - x_1 + vt_1), \quad (2)$$

where $X = x_1 - x_1^{(0)} - vt_1 + vt_1^{(0)}$, v is the propagation velocity and the transmission function $\mathcal{T}(x)$ is

$$\mathcal{T}(x) = \rho_1 \delta(x) + \tau_1 \tau_2 \rho_2 \delta(x - L) + \tau_1 \tau_2 \rho_2^3 \delta(x - 2L) + \dots \quad (3)$$

Therefore, the transmitted wave packet is a superposition of an infinite number of wavelets separated by L . A similar expression holds for the reflected component [47].

The finite width of the wave packet and time delay in reaching the detector give rise to a suppression of interference in the transmission probability $P(1 \rightarrow 1)_{F/B}$. For example, consider a particular case, where one wavelet performed n windings and the other performed m windings. By using Eqs. (2)–(3), one gets two wavelets, $\tau_1 \tau_2 \rho_2^{2n-1} \tilde{\phi}_{s_1}(X + nL)$ and $\tau_1 \tau_2 \rho_2^{2m-1} \tilde{\phi}_{s_1}(X + mL)$. Here, the centers of the wavelets are separated by $|(n - m)L|$. The probability amplitude is given by the superposition of an infinite number of wavelets of the mentioned forms. With increasing difference in the winding numbers $|n - m|$, the interference contribution to the transmission probability is reduced. For a model square wave packet (in momentum space) emitted by a quantum point contact dilutor, the decay function for $n \neq m$ is given as $f(|n - m|) = \frac{i\ell}{L|n - m|} e^{-ik_f L|n - m|} (e^{-i\frac{\ell}{L}|n - m|} - 1)$ where we have $\ell = \frac{v}{eV}$ with V as the bias voltage between the dilutor and the source edge, and v, k_f denote the velocity and the Fermi momentum [47].

Consider next a two-particle process, where each of the sources S_1 and S_2 simultaneously emits one particle. We now consider the case of partial interference between two wave packets and evaluate the probability $P(11)_{F/B}$ that each of the detectors registers one particle. There are two sets of processes which contribute to the two-particle probability amplitude: direct and exchange processes. While for fermions these processes sum up with opposite signs leading to enhanced antibunching, for bosons they add up with same signs. This is a direct manifestation of the statistical exchange phase [1]. More specifically, each exchange process introduces a factor $e^{i\pi\nu}$, with $\nu = 0$ for bosons and $\nu = 1$ for fermions. In the direct process the particle starts from S_1 (S_2) and goes to D_1 (D_2). The two-particle amplitude is $A_{\text{direct}} = \sum_{n,m} A_n^{(1 \rightarrow 1)} A_m^{(2 \rightarrow 2)}$. Direct processes involve an integer number of windings around the anti-dot; a full winding leads to an even number of exchanges and thus the amplitude comes with $+1$ phase for both bosons and fermions, see Eq. (4). In the exchange process the particle starts from S_1 (S_2) goes to D_2 (D_1) and there will be an odd number of exchanges leading to an extra phase, $(-1)^\nu$, Eq. (4). The corresponding amplitude of the exchange processes is $A_{\text{exchange}} = \sum_{n,m} A_{n+\frac{1}{2}}^{(1 \rightarrow 2)} A_{m+\frac{1}{2}}^{(2 \rightarrow 1)}$ [47].

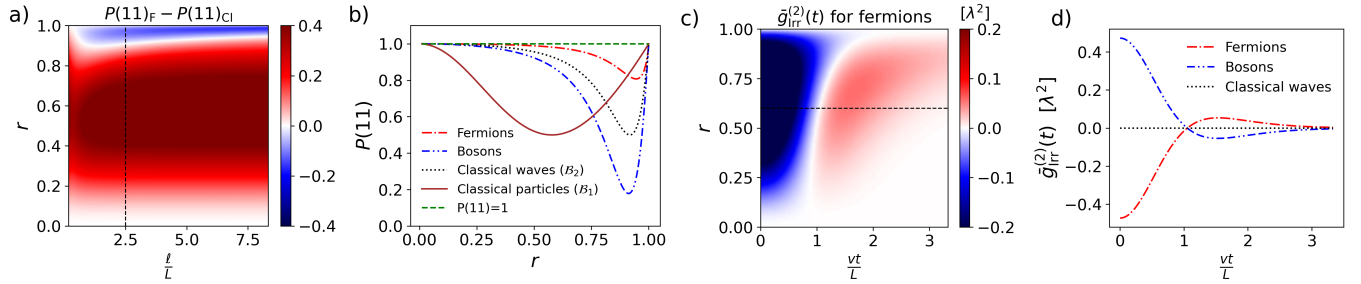


Figure 2. Apparent and truly statistical measures of anti-bunching. (a) Difference between the anti-bunching probabilities $P(11)_F$, Eq. (4) of fermions and $P(11)_{Cl}$ of classical particles as functions of the wave packet width and the edge-QAD reflection amplitude r , Eq. (1). Use of the classical particles as a benchmark shows an apparent bunching of fermions (blue region). We take $k_f = 0$ and $\theta = 0$. (b) Anti-bunching probabilities $P(11)$ for wave packets with $\frac{\ell}{L} = 2.5$ as well as classical particles. Using $P(11)_{Cl}$ for classical particles as a benchmark (\mathcal{B}_1) shows the apparent bunching of fermions near $r = 1$. The classical wave benchmark (\mathcal{B}_2) on the other hand reflects the true quantum statistics of fermions and bosons. (c-d) The irreducible part $\bar{g}_{\text{irr}}^{(2)}(t)$ of the pair-correlation function $\bar{g}^{(2)}(t)$ for a stochastic beam of particles with emission rate λ as function of the detection time difference, t (see Eq. (6) and Sec. VIII B of SM [47]). (c) The function $\bar{g}_{\text{irr}}^{(2)}$ for a dilute stochastic beam of fermions. Due to the extended nature of the collider, $\bar{g}_{\text{irr}}^{(2)}(t)$ may change sign as a function of t , whereas it has a fixed sign in a point-like collider, see Sec. VIII B of SM [47]. (d) For bosons, $\bar{g}_{\text{irr}}^{(2)}$ has the opposite sign from fermions while for classical waves it vanishes. Thus $\bar{g}_{\text{irr}}^{(2)}$ is sensitive to the mutual statistics and hence can probe the statistics. We use $\frac{\ell}{L} = 2.5$, $k_f = 0$, $r = 0.6$, $\theta = 0$ and a finite temperature $\beta^{-1} = eV/75$, see Sec. IV A of SM [47].

The two-particle probability can be written as

$$P(11)_{F/B} = |A_{\text{direct}} + (-1)^\nu A_{\text{exchange}}|^2 \quad (4)$$

where the substitution, $A_n^{(i \rightarrow j)*} A_m^{(k \rightarrow j)} \rightarrow f(|n - m|) A_n^{(i \rightarrow j)*} A_m^{(k \rightarrow j)}$ is to be used to account for interference suppression for the amplitudes to end in the same detector D_j with $j = 1, 2$. With full interference, $f(n) = 1$ for all n , we obtain $P(11)_F = 1$ but generically this is not the case. Partial interference of wave packets emitted from the sources leads to an apparent bunching of fermions [47] for certain values of r , i.e. $\mathcal{Q}_{Cl;F} = P(11)_F - P(11)_{Cl} \leq 0$ (see Fig. 2a-b). Hence, we find that the benchmark, $\mathcal{B}_1 = P(11)_{Cl}$ does not give the correct statistical information. In order to extract two-particle interference terms that reflect mutual statistics, one needs to subtract the contributions from single-particle interference terms. This can be achieved by defining a new benchmark $\mathcal{B}_2 = \mathcal{P}(1 \rightarrow 1)_{s_1} \mathcal{P}(2 \rightarrow 2)_{s_2} + \mathcal{P}(1 \rightarrow 2)_{s_1} \mathcal{P}(2 \rightarrow 1)_{s_2}$, where the subscript denotes the active source, Sec. V of SM [47]. Since \mathcal{B}_2 consists only of single-particle probabilities, it is equivalent to the bunching probability of classical waves; its value falls in between those of bosons and fermions, $P(11)_B < \mathcal{B}_2 < P(11)_F$, see Fig. 2b.

Current correlations.— Next, we show that the antibunching probability $P(11)_{F/B}$, as well as the benchmarks $\mathcal{B}_1, \mathcal{B}_2$ can be accessed by measuring current correlations at the detectors. We begin by noting that the above analysis assumed no more than two particles are present simultaneously in the collider. From an exper-

imental point of view, it is challenging to emit a single wave packet from a source. However, with recent developments in single electron emitters [51–53], one can obtain a dilute stochastic beam of electrons. To model this, we assume that the sources emit Poisson distributed particles with an emission rate λ . The typical distance between emitted particles is v/λ , while the spatial size of the scattered particle (consisting of multiple wavelets) is of order L , giving us the requirement $L \ll v/\lambda$ to not have too many particles in the collider (see Sec. VI of SM [47] for more detailed dependence of this estimate on the reflection amplitude r). Recall also that we obtain partial interference and can treat the collider as extended when the wave packet size is relatively small, $\ell \lesssim L$.

We now account for the fact that the incoming beams represent a mixed state consisting of a Poisson-distributed sequence of particles emitted from the sources (see Sec. VII in SM [47]). Upon entering drain i , a particle passes an ideal detector at a fixed position x_i which tracks the particles that ended up in that drain. The antibunching probability $P(11)_{F/B}$, Eq. (4), can then be expressed in terms of equal time cross-current correlations at the detectors D_1 and D_2 , $\langle I_{d_1} I_{d_2} \rangle \equiv \langle I_{d_1}(t) I_{d_2}(t) \rangle$, normalized by the average currents in the sources $\langle I_{s_i} \rangle = e\lambda$ [47]:

$$P(11)_{F/B} = \frac{\langle I_{d_1} I_{d_2} \rangle_{s_1 s_2}}{\langle I_{s_1} \rangle \langle I_{s_2} \rangle} - \frac{\langle I_{d_1} I_{d_2} \rangle_{s_1}}{\langle I_{s_1} \rangle^2} - \frac{\langle I_{d_1} I_{d_2} \rangle_{s_2}}{\langle I_{s_2} \rangle^2}, \quad (5)$$

where the subscript outside the angular brackets denotes the active source(s). For a chiral channel the current at the detector is given as $I_{d_i}(t) = evn_{d_i}(t)$, where n_{d_i} is the density at the detector. Here, we have subtracted the

correlators with one source turned off because both of the detected particles can come from the same source, a possibility not accounted for in our calculation of $P(11)_{\text{F/B}}$, Eq. (4). Finally, we note that in the limit of a dilute beam, collisions of three or more particles give subleading corrections of order $\lambda L/v$ to Eq. (5).

Information on mutual statistics can be extracted by comparing Eq. (5) with a benchmark. As we discussed above, the appropriate benchmark is $\mathcal{B}_2 = \mathcal{P}(1 \rightarrow 1)_{s_1} \mathcal{P}(2 \rightarrow 2)_{s_2} + \mathcal{P}(1 \rightarrow 2)_{s_1} \mathcal{P}(2 \rightarrow 1)_{s_2}$, which subtracts the contributions from single-particle interference terms. These probabilities can be obtained by measuring average currents at the detectors, e.g. $\mathcal{P}(1 \rightarrow 1)_{s_1} = \langle I_{d_1} \rangle_{s_1} / \langle I_{s_1} \rangle$ and $\mathcal{P}(1 \rightarrow 2)_{s_1} = \langle I_{d_2} \rangle_{s_1} / \langle I_{s_1} \rangle$, see Sec. VII of SM [47]. By subtracting \mathcal{B}_2 from $P(11)_{\text{F/B}}$, Eq. (5) we are only left with the part of $P(11)_{\text{F/B}}$ that is sensitive to quantum statistics.

An extended scatterer can be distinguished from a point-like collider by studying the time resolved $g^{(2)}$ -function [45] which is defined as,

$$\frac{1}{v^2} \bar{g}^{(2)}(t_1, t_2) = \langle n_{d_1}(t_1) n_{d_1}(t_2) \rangle_{s_1 s_2} - \langle n_{d_1}(t_1) n_{d_1}(t_2) \rangle_{s_1} - \langle n_{d_1}(t_1) n_{d_1}(t_2) \rangle_{s_2}, \quad (6)$$

where the $\bar{\cdot}$ indicates averaging over the emission times of the injected beams from the sources S_1, S_2 . Subtracting the auto-correlators with single active source, we prevent counting events where the detected particles are from the same source. Note that, $\bar{g}^{(2)}$ involves averaging over the emission times of the incoming stochastic beam from both the sources. Since this stochastic process is stationary, $\bar{g}^{(2)}(t_1, t_2)$ is a function of only the time difference $t = t_1 - t_2$. Additionally, it includes a reducible part which is equal to $\mathcal{P}(1 \rightarrow 1)_{s_1} \mathcal{P}(1 \rightarrow 2)_{s_1} + \mathcal{P}(2 \rightarrow 2)_{s_2} \mathcal{P}(2 \rightarrow 1)_{s_2}$, Sec. VIII B of SM [47]. By subtracting this reducible part from $\bar{g}^{(2)}(t)$, we obtain the irreducible part, $\bar{g}_{\text{irr}}^{(2)}(t)$ [47]. This time resolved function is a useful tool for distinguishing a point-like scatterer from an extended one (it changes sign as we vary t), Fig. 2c-d. We note that the zero frequency component of $\bar{g}_{\text{irr}}^{(2)}$ is a useful tool for characterizing the mutual statistics, but it falls short of distinguishing a point-like from an extended scatterer.

Discussion.— The analysis presented here focuses on a paradigmatic extended fermionic or bosonic collider, i.e., spatial size L comparative or larger than the wave packet size ℓ . The latter is inversely proportional to the source’s voltage bias. We point out two possible benchmarks of bunching that are identical in the case of a point-like collider but unequal for an extended one. The two candidate benchmarks amount to the antibunching probabilities of either classical particles or classical waves, which are to be subtracted from the measured antibunching probability $P(11)_{\text{F/B}}$, Eq. (5). By using the latter benchmark one removes all the single-particle interference effects and is left with only true quantum statistics information.

While in our model we used chiral channels relevant to quantum Hall edges, historically studies on current correlation measurements and statistics have been extensively investigated in the case of nanowires and impurity scatterers, both in theory and experiment [27, 42, 54–57]. While the present treatment cannot be applied as is to those platforms as it heavily relies on the use of chiral 1D modes, the salient feature that impurities could introduce an internal structure, such as resonant levels, rendering them “extended colliders”. Our model therefore provides an advanced setting for extending the historic studies to include the effects of self-interference.

Note that the presented study excludes the effect of electron-electron interaction. Such interactions indeed affect current correlations present in a collider. Interestingly, one may construct point-like colliders where the effect of interactions is small [58]. Needless to say, one expects the effect of interactions not to be larger for an extended collider.

Extending our work to anyonic platforms is a most intriguing challenge. The reason is the significant contribution of time-domain braiding to auto- and cross-current correlations. In the case of fermions, the correlation functions we define eliminates single-source contributions [58]. Noting that time-domain braiding is essentially a single-source contribution, one has two options: take the same benchmark employed in the case of fermions and end up with time-domain braiding and two-source anyonic contributions, both statistics sensitive. Alternatively, one may try to develop correlators that subtract all single-source contributions (including time-domain braiding) [59]. An ensuing challenging question is to what extent two-source contributions (as opposed to time-domain braiding contribution) are dominant.

One can distinguish a point-like collider from an extended collider by looking at the time-resolved current-correlator at the detector ($g^{(2)}$ -function). With recent developments in the fabrication of innovative geometries on experimental platform in quantum Hall regime [15, 16, 19, 20, 38–41] and single electron emitters [51–53] offer a fertile ground to verify the theoretical predictions. Additionally, the realm of ultracold atoms opens an arena for exploring multiple aspects of our work here—patterning of interference pathways, comparison between bosons and fermions, collisions in a range of settings, and controlled addition and omissions of interactions [60–64].

Acknowledgements.— Y.G. acknowledges support by the DFG Grant MI 658/10-2. Y.G. and J.I.V. acknowledge support by grant no 2022391 from the United States - Israel Binational Science Foundation (BSF), Jerusalem, Israel. Y. G. is supported by the Minerva foundation. Y. G. is an incumbent of InfoSys chair at IISc. S.V. acknowledges the support of the National Science Foundation through Grant No. DMR-2004825.

-
- [1] A. Khare, *Fractional Statistics and Quantum Theory*, 2nd ed. (WORLD SCIENTIFIC, 2005) <https://www.worldscientific.com/doi/pdf/10.1142/5752>.
- [2] J. M. Leinaas and J. Myrheim, *Il Nuovo Cimento B* (1971-1996) **37**, 1 (1977).
- [3] F. Wilczek, *Phys. Rev. Lett.* **49**, 957 (1982).
- [4] S. Rao, “Introduction to abelian and non-abelian anyons,” (2016), [arXiv:1610.09260](https://arxiv.org/abs/1610.09260) [cond-mat.mes-hall].
- [5] C. Nayak, S. H. Simon, A. Stern, M. Freedman, and S. Das Sarma, *Rev. Mod. Phys.* **80**, 1083 (2008).
- [6] D. C. Tsui, H. L. Stormer, and A. C. Gossard, *Phys. Rev. Lett.* **48**, 1559 (1982).
- [7] S. M. Girvin, “The quantum hall effect: Novel excitations and broken symmetries,” (1999), [arXiv:cond-mat/9907002](https://arxiv.org/abs/cond-mat/9907002) [cond-mat.mes-hall].
- [8] D. Arovas, J. R. Schrieffer, and F. Wilczek, *Phys. Rev. Lett.* **53**, 722 (1984).
- [9] C. de C. Chamon, D. E. Freed, S. A. Kivelson, S. L. Sondhi, and X. G. Wen, *Phys. Rev. B* **55**, 2331 (1997).
- [10] K. T. Law, D. E. Feldman, and Y. Gefen, *Phys. Rev. B* **74**, 045319 (2006).
- [11] D. E. Feldman, Y. Gefen, A. Kitaev, K. T. Law, and A. Stern, *Phys. Rev. B* **76**, 085333 (2007).
- [12] P. Bonderson, K. Shtengel, and J. Slingerland, *Annals of Physics* **323**, 2709 (2008).
- [13] D. E. Feldman and B. I. Halperin, *Phys. Rev. B* **105**, 165310 (2022).
- [14] N. Batra, Z. Wei, S. Vishveshwara, and D. E. Feldman, *Phys. Rev. B* **108**, L241302 (2023).
- [15] J. Nakamura, S. Liang, G. C. Gardner, and M. J. Manfra, *Nature Physics* **16**, 931–936 (2020).
- [16] J. Nakamura, S. Fallahi, H. Sahasrabudhe, R. Rahman, S. Liang, G. C. Gardner, and M. J. Manfra, *Nature Physics* **15**, 563 (2019), publisher: Nature Publishing Group.
- [17] J. Nakamura, S. Liang, G. C. Gardner, and M. J. Manfra, *Nature Communications* **13**, 344 (2022).
- [18] J. Nakamura, S. Liang, G. C. Gardner, and M. J. Manfra, *Phys. Rev. X* **13**, 041012 (2023).
- [19] H. K. Kundu, S. Biswas, N. Ofek, V. Umansky, and M. Heiblum, *Nature Physics* **19**, 515–521 (2023).
- [20] I. Neder, N. Ofek, Y. Chung, M. Heiblum, D. Mahalu, and V. Umansky, *Nature* **448**, 333 (2007), publisher: Nature Publishing Group.
- [21] Y. Ronen, T. Werkmeister, D. Haie Najafabadi, A. T. Pierce, L. E. Anderson, Y. J. Shin, S. Y. Lee, Y. H. Lee, B. Johnson, K. Watanabe, T. Taniguchi, A. Yacoby, and P. Kim, *Nature Nanotechnology* **16**, 563 (2021).
- [22] J. Kim, H. Dev, R. Kumar, A. Ilin, A. Haug, V. Bhardwaj, C. Hong, K. Watanabe, T. Taniguchi, A. Stern, and Y. Ronen, *Nature Nanotechnology* (2024), [10.1038/s41565-024-01751-w](https://doi.org/10.1038/s41565-024-01751-w).
- [23] T. Werkmeister, J. R. Ehrets, Y. Ronen, M. E. Wesson, D. Najafabadi, Z. Wei, K. Watanabe, T. Taniguchi, D. E. Feldman, B. I. Halperin, A. Yacoby, and P. Kim, *Nature Communications* **15**, 6533 (2024).
- [24] T. Werkmeister, J. R. Ehrets, M. E. Wesson, D. H. Najafabadi, K. Watanabe, T. Taniguchi, B. I. Halperin, A. Yacoby, and P. Kim, “Anyon braiding and telegraph noise in a graphene interferometer,” (2024), [arXiv:2403.18983](https://arxiv.org/abs/2403.18983) [cond-mat.mes-hall].
- [25] D. T. McClure, W. Chang, C. M. Marcus, L. N. Pfeiffer, and K. W. West, *Phys. Rev. Lett.* **108**, 256804 (2012).
- [26] N. L. Samuelson, L. A. Cohen, W. Wang, S. Blanch, T. Taniguchi, K. Watanabe, M. P. Zaletel, and A. F. Young, “Anyonic statistics and slow quasiparticle dynamics in a graphene fractional quantum hall interferometer,” (2024), [arXiv:2403.19628](https://arxiv.org/abs/2403.19628) [cond-mat.mes-hall].
- [27] Y. Blanter and M. Büttiker, *Physics Reports* **336**, 1–166 (2000).
- [28] I. Safi, P. Devillard, and T. Martin, *Phys. Rev. Lett.* **86**, 4628 (2001).
- [29] R. Guyon, T. Martin, I. Safi, and P. Devillard, *Comptes Rendus Physique* **3**, 697 (2002).
- [30] S. Vishveshwara, *Phys. Rev. Lett.* **91**, 196803 (2003).
- [31] E.-A. Kim, M. Lawler, S. Vishveshwara, and E. Fradkin, *Phys. Rev. Lett.* **95**, 176402 (2005).
- [32] E.-A. Kim, M. J. Lawler, S. Vishveshwara, and E. Fradkin, *Phys. Rev. B* **74**, 155324 (2006).
- [33] G. Campagnano, O. Zilberberg, I. V. Gornyi, D. E. Feldman, A. C. Potter, and Y. Gefen, *Phys. Rev. Lett.* **109**, 106802 (2012).
- [34] G. Campagnano, O. Zilberberg, I. V. Gornyi, and Y. Gefen, *Phys. Rev. B* **88**, 235415 (2013).
- [35] B. Rosenow, I. P. Levkivskyi, and B. I. Halperin, *Phys. Rev. Lett.* **116**, 156802 (2016).
- [36] J.-Y. M. Lee and H.-S. Sim, *Nature Communications* **13** (2022), [10.1038/s41467-022-34329-y](https://doi.org/10.1038/s41467-022-34329-y).
- [37] C. Han, J. Park, Y. Gefen, and H.-S. Sim, *Nature Communications* **7** (2016), [10.1038/ncomms11131](https://doi.org/10.1038/ncomms11131).
- [38] H. Bartolomei, M. Kumar, R. Bisognin, A. Marguerite, J.-M. Berroir, E. Bocquillon, B. Plaçais, A. Cavanna, Q. Dong, U. Gennser, Y. Jin, and G. Fève, *Science* **368**, 173 (2020).
- [39] M. Ruelle, E. Frigerio, J.-M. Berroir, B. Plaçais, J. Rech, A. Cavanna, U. Gennser, Y. Jin, and G. Fève, *Phys. Rev. X* **13**, 011031 (2023).
- [40] J.-Y. M. Lee, C. Hong, T. Alkalay, N. Schiller, V. Umansky, M. Heiblum, Y. Oreg, and H.-S. Sim, *Nature* **617**, 277–281 (2023).
- [41] E. Bocquillon, V. Freulon, J.-M. Berroir, P. Degiovanni, B. Plaçais, A. Cavanna, Y. Jin, and G. Fève, *Science* **339**, 1054 (2013), publisher: American Association for the Advancement of Science.
- [42] M. Büttiker, *Phys. Rev. B* **46**, 12485 (1992).
- [43] S. Barbarino, R. Fazio, V. Vedral, and Y. Gefen, *Phys. Rev. B* **99**, 045430 (2019).
- [44] Here reducible refers to all the contributions to the cross/auto-correlations with just a single active source.
- [45] R. Loudon, *The Quantum Theory of Light* (Oxford University Press, 2000).
- [46] N. Schiller, Y. Shapira, A. Stern, and Y. Oreg, *Phys. Rev. Lett.* **131**, 186601 (2023).
- [47] See Supplementary Material for more details.
- [48] By ‘classical’, we mean in this paper the complete lack of interference, still allowing for tunneling processes.
- [49] G. Baym, *Lectures On Quantum Mechanics (1st ed.)* (CRC Press, 1969).
- [50] I. V. Krainov, A. P. Dmitriev, and N. S. Averkiev, *Phys. Rev. B* **106**, 245421 (2022).
- [51] S. Ol’khovskaya, J. Splettstoesser, M. Moskalets, and M. Büttiker, *Phys. Rev. Lett.* **101**, 166802 (2008).
- [52] J. Dubois, T. Jullien, F. Portier, P. Roche, A. Cavanna, Y. Jin, W. Wegscheider, P. Roulleau, and D. C. Glattli, *Nature* **502**, 659 (2013).

- [53] W. D. Oliver, J. Kim, R. C. Liu, and Y. Yamamoto, *Science* **284**, 299 (1999).
- [54] A. Crépieux, R. Guyon, P. Devillard, and T. Martin, *Phys. Rev. B* **67**, 205408 (2003).
- [55] S. Pugnetti, F. Dolcini, D. Bercioux, and H. Grabert, *Phys. Rev. B* **79**, 035121 (2009).
- [56] L. G. Herrmann, F. Portier, P. Roche, A. L. Yeyati, T. Kontos, and C. Strunk, *Phys. Rev. Lett.* **104**, 026801 (2010).
- [57] L. Hofstetter, S. Csonka, J. Nygård, and C. Schönberger, *Nature* **461**, 960 (2009).
- [58] G. Zhang, C. Hong, T. Alkalay, V. Umansky, M. Heiblum, I. Gornyi, and Y. Gefen, *Nature Communications* **15**, 3428 (2024).
- [59] G. Zhang, P. Glidic, F. Pierre, I. Gornyi, and Y. Gefen, “Fractional-statistics-induced entanglement from andreev-like tunneling,” (2023), arXiv:2312.16556 [cond-mat.mes-hall].
- [60] C.-C. Chien, M. Zwolak, and M. Di Ventra, *Phys. Rev. A* **85**, 041601 (2012).
- [61] C.-C. Chien, S. Peotta, and M. Di Ventra, *Nature Physics* **11**, 998 (2015).
- [62] Y. Nishida, *Phys. Rev. A* **93**, 011606 (2016).
- [63] J. Yago Malo, E. P. L. van Nieuwenburg, M. H. Fischer, and A. J. Daley, *Phys. Rev. A* **97**, 053614 (2018).
- [64] S. Nakada, S. Uchino, and Y. Nishida, *Phys. Rev. A* **102**, 031302 (2020).

Supplemental Materials: Interplay of quantum statistics and self-interference in extended colliders

In this supplementary material, we show the details of results discussed in the article. We begin by giving the scattering formalism of our calculations in Sec. I, which are independent of the shape of the wave packet that we choose and hence are applicable to all finite spatial width wave packets. In the following section, Sec. II we demonstrate the differences between the point-like collider and the proposed extended collider. We show the differences between single-particle scattering and two-particle scattering in the two types of colliders. In the next section, Sec. III, we explain the origin of apparent bunching of fermions using a toy-model and show that its origin is related to the self-interfering single-particle trajectories (histories). In the section, Sec. IV, we start by discussing wave packets and show that finite spatial width (of the wave packet) leads to partial interference. We also discuss a dilute quantum point contact (QPC), which emits a dilute stochastic beam of particles (wave packets). In the following section, Sec. V we define a benchmark for extracting the true mutual statistics of the colliding particles from the two-particle probabilities. The section, Sec. VI gives the spatial width of the reflected and transmitted wave packet in the detector drains. Since we work with a stochastic beam of particles from the sources and our calculations are restricted to at most two particles simultaneously in the collider, we determine the appropriate emission rate λ to have not more than two particles simultaneously in the collider. In the section, Sec. VII we calculate the cross-current correlator for a dilute stochastic beam of particles, and by defining a new benchmark in terms of the average currents, we extract the true statistics of the particles. In the final section, Sec. VIII, we give a pedagogical definition of the $g^{(2)}$ -function and then generalize it for a stochastic beam of particles denoted by $\bar{g}^{(2)}$. We demonstrate that the $\bar{g}^{(2)}$ -function can be accessed experimentally by studying the auto-correlation of currents at a given detector. Finally, by defining an irreducible $\bar{g}^{(2)}$, referred to as $\bar{g}_{\text{irr}}^{(2)}$, we show that this time resolved function differentiate an extended collider from a point-like collider. Also, we demonstrate that the zero-frequency Fourier transform of $\bar{g}_{\text{irr}}^{(2)}$ gives information on the mutual statistics of the particles.

I. SCATTERING FORMALISM

In the setup, we have two chiral edges, with left moving particles on the lower edge and right moving particles on the upper edge. The chiral edges have linear dispersion, and the Hamiltonian of the system with right and left moving particles is given as,

$$\mathcal{H} = \int_{-\infty}^{\infty} dx \psi^\dagger (-iv\sigma_z \partial_x) \psi(x), \quad (\text{S1})$$

where v is the magnitude of the velocity of the particles and for simplicity we work in the units $\hbar = 1$. The field operator $\psi(x)$ is given as,

$$\psi^\dagger(x) = \int_{-\infty}^{\infty} \frac{dk}{\sqrt{2\pi}} \begin{pmatrix} c_{k,R}^\dagger e^{-ikx} \\ c_{k,L}^\dagger e^{ikx} \end{pmatrix}. \quad (\text{S2})$$

and $c_{k,R}^\dagger$ is the annihilation operator for the right movers and $c_{k,L}^\dagger$ is the annihilation operator for the left moving particles and satisfy the anti-commutation relations, $\{c_{k,L}, c_{k',L}^\dagger\} = 2\pi\delta(k - k') = \{c_{k,R}, c_{k',R}^\dagger\}$ and $\{c_{k,L}, c_{k',R}^\dagger\} = 0$.

The collider, Fig. 1a consists of two sources (S_1, S_2) and two detectors (D_1, D_2). At position, $x = 0$, we have a collider characterized by a S -matrix. On the left side (L) of the collider ($x < 0$), we have, c_{k,s_1}^\dagger , creation operator for right moving particle coming from the source, S_1 and c_{k,d_2}^\dagger , creation operator for the left moving particle going into D_2 . Correspondingly, on the right side (R) of the collider ($x > 0$), we have c_{k,s_2}^\dagger for a left moving particle coming from S_2 and c_{k,d_1}^\dagger for a right moving particle, going into the detector, D_1 . Hamiltonian of the proposed setup, Fig. 1a, can be written as the sum of Hamiltonians on the left side of collider (\mathcal{H}_L) and right side of the collider (\mathcal{H}_R), i.e.,

$$\mathcal{H} = \mathcal{H}_L + \mathcal{H}_R, \quad (\text{S3})$$

where,

$$\mathcal{H}_L = \int_{-\infty}^0 dx \psi_L^\dagger(x) (-iv\sigma_z) \psi_L(x) \quad \text{and} \quad \psi_L^\dagger(x) = \int_{-\infty}^{\infty} \frac{dk}{\sqrt{2\pi}} \begin{pmatrix} c_{k,s_1}^\dagger e^{-ikx} \\ c_{k,d_2}^\dagger e^{ikx} \end{pmatrix}, \quad (\text{S4})$$

$$\mathcal{H}_R = \int_0^{\infty} dx \psi_R^\dagger(x) (-iv\sigma_z) \psi_R(x) \quad \text{and} \quad \psi_R^\dagger(x) = \int_{-\infty}^{\infty} \frac{dk}{\sqrt{2\pi}} \begin{pmatrix} c_{k,d_1}^\dagger e^{-ikx} \\ c_{k,s_2}^\dagger e^{ikx} \end{pmatrix}. \quad (\text{S5})$$

Once we have defined the creation/annihilation operators at the sources and detectors, these are related to each other by the unitary S -matrix of the collider:

$$\begin{pmatrix} c_{d_1,k} \\ c_{d_2,k} \end{pmatrix} = \begin{pmatrix} \mathcal{T}_k & \mathcal{R}_k \\ \mathcal{R}_k & \mathcal{T}_k \end{pmatrix} \begin{pmatrix} c_{s_1,k} \\ c_{s_2,k} \end{pmatrix}, \quad (\text{S6})$$

where the full expression for \mathcal{T}_k and \mathcal{R}_k are given later in Sec. II B (note that the S -matrix is momentum-dependent which is a result of non-point-like geometry of the collider, Fig. 1a).

In order to familiarize with the formalism, we start by understanding the single-particle physics and consider a specific example, where we create a wave packet at source S_1 and calculate the amplitude to find the particle in the detector, D_1 . The operator $\tilde{\phi}_{s_1}^\dagger$, creates a wave packet at $(x_1^{(0)}, t_1^{(0)})$ originating from S_1 and is given as,

$$\tilde{\phi}_{s_1}^\dagger(x_1^{(0)}, t_1^{(0)}) = \int_{-\infty}^{\infty} dk e^{ik(-x_1^{(0)} + vt_1^{(0)})} \phi^*(k) c_{k,s_1}^\dagger, \quad (\text{S7})$$

where $\phi(k)$ is the wave form in momentum space, normalized such that $\int_{-\infty}^{\infty} dk |\phi(k)|^2 = 1$. The creation operator at position (x_1, t_1) in the detector lead (D_1) is given as,

$$\phi_{d_1}^\dagger(x_1, t_1) = \int_{-\infty}^{\infty} \frac{dk}{\sqrt{2\pi}} e^{ik(-x_1 + vt_1)} c_{k,d_1}^\dagger. \quad (\text{S8})$$

The amplitude for propagation to D_1 is

$$A(S_1 \rightarrow D_1) = \langle \phi_{d_1}(x_1, t_1) \tilde{\phi}_{s_1}^\dagger(x_1^{(0)}, t_1^{(0)}) \rangle, \quad (\text{S9})$$

$$= \int_{-\infty}^{\infty} \frac{dk}{\sqrt{2\pi}} \phi^*(k) \mathcal{T}_k e^{ik(x_1 - x_1^{(0)} - vt_1 + vt_1^{(0)})}, \quad (\text{S10})$$

where we have used Eq. (S6) and the expectation value is taken with respect to a state $|\Omega\rangle$, which is a filled Fermi-sea at zero temperature. For calculating the probability from the amplitude, we integrate over the detection time t_1 , from $t_1^{(0)}$ to ∞ in order to ensure that the particle has reached the detector:

$$\mathcal{P}(S_1 \rightarrow D_1) = \int_{t_1^{(0)}}^{\infty} v dt_1 |A(S_1 \rightarrow D_1)|^2. \quad (\text{S11})$$

Now, note that we have wave packets and because of causality, particle reaches the detector only after the time, $t_1^{(0)}$. The amplitude of finding the the particle at the detector for $t < t_1^{(0)}$ is zero and therefore we can effectively replace the lower limit of integration from $t_1^{(0)}$ to $-\infty$. Hence, we have,

$$\mathcal{P}(S_1 \rightarrow D_1) = \int_{-\infty}^{\infty} v dt_1 |A(S_1 \rightarrow D_1)|^2 = \int_{-\infty}^{\infty} dk |\mathcal{T}_k|^2 |\phi(k)|^2. \quad (\text{S12})$$

Similarly, we obtain the probability of being detected in D_2 ,

$$\mathcal{P}(S_1 \rightarrow D_2) = \int_{-\infty}^{\infty} dk |\mathcal{R}_k|^2 |\phi(k)|^2. \quad (\text{S13})$$

Using the above scheme, we calculate the detection probabilities for point-like collider and extended collider in the following sections. For simplicity in the notations, we would like to denote the single-particle probability from the source to drain as $\mathcal{P}(i \rightarrow j)$ instead of $\mathcal{P}(S_i \rightarrow D_j)$ and amplitudes as $A(i \rightarrow j)$ instead of $A(S_i \rightarrow D_j)$.

II. ANTIBUNCHING PROBABILITY $P(11)$ IN POINT-LIKE AND EXTENDED COLLIDERS

In this section we are going to elaborate on the characteristic differences between a point-like and an extended collider. We begin by discussing single-particle physics and then two-particle physics.

A. Single-particle scattering in a point-like collider

In a point-like collider the S -matrix is momentum independent and is given as,

$$S = \begin{pmatrix} \mathcal{T} & \mathcal{R} \\ \mathcal{R} & \mathcal{T} \end{pmatrix}. \quad (\text{S14})$$

Once the wave packet goes through the collider, a part of every incoming wave packet will go to the lead with detector D_1 (transmission) and other part will go to lead with D_2 (reflection). Lets focus on the transmitted wave packet and assume x_1 be the location of the detector, D_1 . Transmitted wave packet is related to the incoming one via the S -matrix, Eq. (S14). Transmission amplitude is,

$$A(1 \rightarrow 1) = \langle \phi_{d_1}(x_1, t_1) \tilde{\phi}_{s_1}^\dagger(x_1^{(0)}, t_1^{(0)}) \rangle = \int_{-\infty}^{\infty} \frac{dk}{\sqrt{2\pi}} \mathcal{T} e^{ik(x_1 - x_1^{(0)} - vt_1 + vt_1^{(0)})} \phi^*(k), \quad (\text{S15})$$

with $\phi_{d_1}^\dagger(x_1, t_1) = \int_{-\infty}^{\infty} dk e^{ik(-x_1 + vt_1)} c_{k, d_1}^\dagger$ is the creation operator in the detector lead at (x_1, t_1) and the expectation is with respect to the filled Fermi-state, $|\Omega\rangle$. Since our S -matrix parameters in the point-like collider are not momentum dependent and therefore we can pull out the \mathcal{T} from the integration. To obtain the detection probability, we integrate over all possible detection time, t_1 ,

$$\mathcal{P}(1 \rightarrow 1) = \int_{t_1^{(0)}}^{\infty} v dt_1 |A(1 \rightarrow 1)|^2. \quad (\text{S16})$$

By using the argument of causality as in the previous section, Sec. I, we can effectively replace the lower limit $t_1^{(0)}$ with $-\infty$. This implies,

$$\mathcal{P}(1 \rightarrow 1) = \int_{-\infty}^{\infty} v dt_1 |A(1 \rightarrow 1)|^2, \quad (\text{S17})$$

$$= \int_{-\infty}^{\infty} \frac{v dt_1}{2\pi} |\mathcal{T}|^2 \int_{-\infty}^{\infty} dk_1 \int_{-\infty}^{\infty} dk_2 e^{-ik_1(x_1 - x_1^{(0)} - vt_1 + vt_1^{(0)})} e^{ik_2(x_1 - x_1^{(0)} - vt_1 + vt_1^{(0)})} \phi(k_1) \phi^*(k_2). \quad (\text{S18})$$

By performing the time integral first we get $\delta(k_1 - k_2)$ and this can be simplified to,

$$\mathcal{P}(1 \rightarrow 1) = \int_{-\infty}^{\infty} dk |\phi(k)|^2 |\mathcal{T}|^2, \quad (\text{S19})$$

$$= |\mathcal{T}|^2. \quad (\text{S20})$$

Here, our transmission amplitude is independent of momentum and therefore we can take it out of the integration. Hence, the probability of transmission is equal to $|\mathcal{T}|^2$ and similarly, one finds $\mathcal{P}(1 \rightarrow 2) = |\mathcal{R}|^2$.

B. Single-particle scattering in an extended collider

Extended collider is realized with the following effective S -matrix that we calculate using geometric series,

$$S = \begin{pmatrix} \mathcal{T}_k & \mathcal{R}_k \\ \mathcal{R}_k & \mathcal{T}_k \end{pmatrix} = \begin{pmatrix} \rho_1 + \frac{\tau_1 \tau_2 \rho_2 e^{ikL}}{1 - \rho_2^2 e^{ikL}} & \frac{\tau_1 \tau_2 e^{\frac{ikL}{2}}}{1 - \rho_2^2 e^{ikL}} \\ \frac{\tau_1 \tau_2 e^{\frac{ikL}{2}}}{1 - \rho_2^2 e^{ikL}} & \rho_1 + \frac{\tau_1 \tau_2 \rho_2 e^{ikL}}{1 - \rho_2^2 e^{ikL}} \end{pmatrix} = \begin{pmatrix} \frac{r e^{i\theta} [1 - e^{ikL - 2i\theta}]}{1 - r^2 e^{ikL - i2\theta}} & -\frac{(1 - r^2) e^{i\frac{kL}{2}}}{1 - r^2 e^{ikL - i2\theta}} \\ -\frac{(1 - r^2) e^{i\frac{kL}{2}}}{1 - r^2 e^{ikL - i2\theta}} & \frac{r e^{i\theta} [1 - e^{ikL - 2i\theta}]}{1 - r^2 e^{ikL - i2\theta}} \end{pmatrix}. \quad (\text{S21})$$

where ρ_1, ρ_2 are the amplitude to remain on the edge or in the quantum anti-dot (QAD) and τ_1, τ_2 are the amplitude to hop in/out of the QAD at each junction in the extended collider, Eq. (1). The transmission amplitude, \mathcal{T}_k in the effective S -matrix, Eq. (S21) is obtained by the geometric series of all the possible processes, Fig. S1a,

$$\mathcal{T}_k = \rho_1 + \tau_1 \tau_2 \rho_2 e^{ikL} + \tau_1 \tau_2 \rho_2^3 e^{2ikL} + \dots = \rho_1 + \frac{\tau_1 \tau_2 \rho_2 e^{ikL}}{1 - \rho_2^2 e^{ikL}}. \quad (\text{S22})$$

As a result, for an extended collider, we get,

$$A(1 \rightarrow 1) = \langle \phi_{d_1}(x_1, t_1) \tilde{\phi}_{s_1}^\dagger(x_1^0, t_1^0) \rangle = \int_{-\infty}^{\infty} \frac{dk}{\sqrt{2\pi}} \mathcal{T}_k e^{ik(x_1 - x_1^{(0)} - vt_1 + vt_1^{(0)})} \phi(k)^*, \quad (\text{S23})$$

$$= \rho_1 \int_{-\infty}^{\infty} \frac{dk}{\sqrt{2\pi}} e^{ik(x_1 - x_1^{(0)} - vt_1 + vt_1^{(0)})} \phi(k)^* \quad (\text{S24})$$

$$+ \rho_2 \tau_1 \tau_2 \int_{-\infty}^{\infty} \frac{dk}{\sqrt{2\pi}} e^{ik(x_1 - x_1^{(0)} - vt_1 + vt_1^{(0)} + kL)} \phi(k)^* + \dots \quad (\text{S25})$$

$$= \int_{-\infty}^{\infty} dx \tilde{\phi}_{s_1}(x - x_1^{(0)} + vt_1^{(0)}) \mathcal{T}(x - x_1 + vt_1) \quad (\text{S26})$$

where we have defined the following,

$$\tilde{\phi}_{s_1}(x) = \int_{-\infty}^{\infty} dk e^{ik(x - x_1^{(0)} + vt_1^{(0)})} \phi^*(k) \quad (\text{S27})$$

$$\mathcal{T}(x) = \rho_1 \delta(x) + \tau_1 \tau_2 \rho_2 \delta(x - L) + \tau_1 \tau_2 \rho_2^3 \delta(x - 2L) + \dots \quad (\text{S28})$$

and one obtains Eq. (3) in the main text. This implies, we get an infinite number of wavelets in the transmission lead. Each of the wavelet have reduced amplitude and are separated by L , size of the detector, Fig. 1a. From here the probability is calculated as,

$$\mathcal{P}(1 \rightarrow 1) = \int_{t_1^{(0)}}^{\infty} v dt_1 |A(S_1 \rightarrow D_1)|^2 = \int_{-\infty}^{\infty} \frac{v dt_1}{2\pi} \left| \int_{-\infty}^{\infty} dk \mathcal{T}_k e^{ik(x_1 - x_1^{(0)} - vt_1 + vt_1^{(0)})} \phi^*(k) \right|^2, \quad (\text{S29})$$

$$= \int_{-\infty}^{\infty} dk |\mathcal{T}_k|^2 |\phi(k)|^2. \quad (\text{S30})$$

In the limit where the spatial width of the wave packet is much smaller than the size of the QAD, L , then the amplitudes A_0, A_1, \dots in Eq. (S25) are well localized in position space separated by L . Therefore the interference terms like, $A_n^* A_m \rightarrow 0$ for $n \neq m$ and hence it reproduces the result for classical particles (subscript ‘‘CI’’ denotes the classical particles),

$$\mathcal{P}(1 \rightarrow 1)_{\text{CI}} = |\rho_1|^2 + \frac{|\tau_1|^2 |\tau_2|^2 |\rho_2|^2}{1 - |\rho_2|^4} = \frac{2r^2}{1 + r^2}. \quad (\text{S31})$$

1. Non-identical S -matrix at each channel-QAD junction

We would like to finish this subsection by commenting on the case where the two junctions S -matrix are different. Let us consider the case where the upper junction is parameterized by (r_1, θ_1) and let the lower junction be parameterized by (r_2, θ_2) , Eq. (1). Consider a single particle coming from the source S_1 and let us assume that the particle

have momentum k . As a result of this, the effective matrix is modified in this case. Let us denote the new effective matrix with $S_{\text{Non-identical junction}}$,

$$S_{\text{Non-identical junction}} = \begin{pmatrix} \frac{e^{i\theta_1}[r_1 - r_2 e^{i(kL - \theta_1 - \theta_2)}]}{1 - r_1 r_2 e^{i(kL - \theta_1 - \theta_2)}} & -\frac{\sqrt{(1-r_1^2)(1-r_2^2)} e^{ikL/2}}{1 - r_1 r_2 e^{i(kL - \theta_1 - \theta_2)}} \\ -\frac{\sqrt{(1-r_1^2)(1-r_2^2)} e^{ikL/2}}{1 - r_1 r_2 e^{i(kL - \theta_1 - \theta_2)}} & \frac{e^{i\theta_1}[r_1 - r_2 e^{i(kL - \theta_1 - \theta_2)}]}{1 - r_1 r_2 e^{i(kL - \theta_1 - \theta_2)}} \end{pmatrix} \quad (\text{S32})$$

Hence, we find that the effective S -matrix in the case of non-identical channel-QAD junctions also respects Time-reversal symmetry as in the identical case. From here, we compute the single-particle probability of transmission with a definite momentum k is given as,

$$\mathcal{P}_k(1 \rightarrow 1) = \mathcal{P}_k(2 \rightarrow 2) = \left| [S_{\text{Non-identical junction}}]_{11} \right|^2, \quad (\text{S33})$$

$$= \frac{r_1^2 + r_2^2 - 2r_1 r_2 \cos(kL - \theta_1 - \theta_2)}{1 - 2r_1 r_2 \cos(kL - \theta_1 - \theta_2) + r_1^2 r_2^2}. \quad (\text{S34})$$

Similarly, the probability of reflection is given as,

$$\mathcal{P}_k(1 \rightarrow 2) = \mathcal{P}_k(2 \rightarrow 1) = \left| [S_{\text{Non-identical junction}}]_{12} \right|^2, \quad (\text{S35})$$

$$= \frac{(1 - r_1^2)(1 - r_2^2)}{1 - 2r_1 r_2 \cos(kL - \theta_1 - \theta_2) + r_1^2 r_2^2}. \quad (\text{S36})$$

In the case when we have identical junctions, we have resonant tunneling [49] in the system, $\mathcal{P}(1 \rightarrow 2) = \mathcal{P}(2 \rightarrow 1) = 1$ for $kL = 2\theta$, which is no more the case with different S -matrix at the junctions.

C. Two-particle scattering in a point-like collider

The two-particle probability can be computed in a similar way, we assume the detector D_1 is located at x_1 and detector D_2 is at x_2 ,

$$A(11)_{\text{B/F}} = \langle \phi_{d_1}(x_1, t_1) \phi_{d_2}(x_2, t_2) \tilde{\phi}_{s_2}^\dagger(x_2^{(0)}, t_2^{(0)}) \tilde{\phi}_{s_1}^\dagger(x_1^{(0)}, t_1^{(0)}) \rangle, \quad (\text{S37})$$

$$= \langle \phi_{d_1}(x_1, t_1) \tilde{\phi}_{s_1}^\dagger(x_1^{(0)}, t_1^{(0)}) \rangle \langle \phi_{d_2}(x_2, t_2) \tilde{\phi}_{s_2}^\dagger(x_2^{(0)}, t_2^{(0)}) \rangle, \quad (\text{S38})$$

$$\pm \langle \phi_{d_1}(x_1, t_1) \tilde{\phi}_{s_2}^\dagger(x_2^{(0)}, t_2^{(0)}) \rangle \langle \phi_{d_2}(x_2, t_2) \tilde{\phi}_{s_1}^\dagger(x_1^{(0)}, t_1^{(0)}) \rangle, \quad (\text{S39})$$

$$= A_{\text{direct}} \pm A_{\text{exchange}}. \quad (\text{S40})$$

Now, in order to get the probability for two-particle event, we integrate the detection time from $t_0 = \min\{t_1^{(0)}, t_2^{(0)}\}$ to ∞ ,

$$P(11)_{\text{B/F}} = \int_{t_0}^{\infty} \int_{t_0}^{\infty} v^2 dt_1 dt_2 |A_{\text{direct}} \pm A_{\text{exchange}}|^2. \quad (\text{S41})$$

Since, in the case of point-like collider, the transmission and reflection amplitude are independent of the momentum and the unitarity of the S -matrix, Eq. (S14) implies,

$$S^\dagger S = \mathbb{I}, \quad (\text{S42})$$

$$\Rightarrow |\mathcal{R}|^2 + |\mathcal{T}|^2 = 1 \quad \text{and} \quad \mathcal{R}^* \mathcal{T} + \mathcal{T}^* \mathcal{R} = 0. \quad (\text{S43})$$

In the probability, $P(11)_{\text{B/F}}$, there are terms proportional to $\mathcal{T}^{*2} \mathcal{R}^2$ and then by using Eq. (S43), we get, $\mathcal{T}^{*2} \mathcal{R}^2 = -|\mathcal{R}|^2 |\mathcal{T}|^2$ and hence we obtain,

$$P(11)_{\text{B/F}} = |\mathcal{R}|^4 + |\mathcal{T}|^4 \mp 2|J|^2 |\mathcal{R}|^2 |\mathcal{T}|^2, \quad \text{where} \quad J = \int_{-\infty}^{\infty} dk e^{ik(x_2^{(0)} + vt_2^{(0)} + x_1^{(0)} - vt_1^{(0)})} |\phi(k)|^2. \quad (\text{S44})$$

Function J is the overlap function [27], when the particles arrive at the collider at the same time, i.e, $x_2^{(0)} + vt_2^{(0)} + x_1^{(0)} - vt_1^{(0)} = 0$ then, $J = 1$. In the case with fermions arriving simultaneously in the collider, by Pauli's principle we expect them to leave for different detectors and consistently we also obtain $P(11)_{\text{F}} = 1$.

D. Two-particle scattering in an extended collider

Characteristic feature of extended collider is the momentum dependent transmission and reflection coefficients in the effective S -matrix of the collider, Eq. (S21). As a result, we get a train of wavelets in the drains, Eq. (S25). With detector D_1 at x_1 and D_2 at x_2 , the amplitudes for direct and exchange processes are given as follows,

$$A_{\text{direct}} = \langle \phi_{d_1}(x_1, t_1) \tilde{\phi}_{s_1}^\dagger(x_1^{(0)}, t_1^{(0)}) \rangle \langle \phi_{d_2}(x_2, t_2) \tilde{\phi}_{s_2}^\dagger(x_2^{(0)}, t_2^{(0)}) \rangle, \quad (\text{S45})$$

$$= \mathcal{I}_1(x_1, t_1; x_1^{(0)}, t_1^{(0)}) \mathcal{I}_2(x_2, t_2; x_2^{(0)}, t_2^{(0)}), \quad (\text{S46})$$

$$A_{\text{exchange}} = \langle \phi_{d_1}(x_1, t_1) \tilde{\phi}_{s_2}^\dagger(x_2^{(0)}, t_2^{(0)}) \rangle \langle \phi_{d_2}(x_2, t_2) \tilde{\phi}_{s_1}^\dagger(x_1^{(0)}, t_1^{(0)}) \rangle, \quad (\text{S47})$$

$$= \mathcal{J}_2(x_1, t_1; x_2^{(0)}, t_2^{(0)}) \mathcal{J}_1(x_2, t_2; x_1^{(0)}, t_1^{(0)}), \quad (\text{S48})$$

where,

$$\mathcal{I}_1(x_1, t_1; x_1^{(0)}, t_1^{(0)}) = \int_{-\infty}^{\infty} \frac{dk_3}{\sqrt{2\pi}} e^{ik_3(x_1 - vt_1 - x_1^{(0)} + vt_1^{(0)})} \phi^*(k_3) \mathcal{T}_{k_3}, \quad (\text{S49})$$

$$\mathcal{I}_2(x_2, t_2; x_2^{(0)}, t_2^{(0)}) = \int_{-\infty}^{\infty} \frac{dk_2}{\sqrt{2\pi}} e^{ik_2(-x_2 - vt_2 + x_2^{(0)} + t_2^{(0)})} \phi^*(k_2) \mathcal{T}_{k_2}, \quad (\text{S50})$$

$$\mathcal{J}_1(x_2, t_2; x_1^{(0)}, t_1^{(0)}) = \int_{-\infty}^{\infty} \frac{dk_1}{\sqrt{2\pi}} e^{ik_1(-x_2 - vt_2 - x_1^{(0)} + t_1^{(0)})} \phi^*(k_1) \mathcal{R}_{k_1}, \quad (\text{S51})$$

$$\mathcal{J}_2(x_1, t_1; x_2^{(0)}, t_2^{(0)}) = \int_{-\infty}^{\infty} \frac{dk_2}{\sqrt{2\pi}} e^{ik_2(x_1 - vt_1 + x_2^{(0)} + t_2^{(0)})} \phi^*(k_2) \mathcal{R}_{k_2}. \quad (\text{S52})$$

The probability in this case is,

$$P(11)_{\text{B/F}} = \int_{-\infty}^{\infty} \int_{-\infty}^{\infty} v^2 dt_1 dt_2 |\mathcal{I}_1(x_1, t_1; x_1^{(0)}, t_1^{(0)}) \mathcal{I}_2(x_2, t_2; x_2^{(0)}, t_2^{(0)}) \pm \mathcal{J}_2(x_1, t_1; x_2^{(0)}, t_2^{(0)}) \mathcal{J}_1(x_2, t_2; x_1^{(0)}, t_1^{(0)})|^2. \quad (\text{S53})$$

where, we have the lower limit by of the integration as $-\infty$ by using the arguments in section Sec. I. Further, we get,

$$P(11)_{\text{B/F}} = \int_{-\infty}^{\infty} v dt_1 |\mathcal{I}_1(x_1, t_1; x_1^{(0)}, t_1^{(0)})|^2 \int_{-\infty}^{\infty} v dt_2 |\mathcal{I}_2(x_2, t_2; x_2^{(0)}, t_2^{(0)})|^2, \quad (\text{S54})$$

$$+ \int_{-\infty}^{\infty} v dt_1 |\mathcal{J}_2(x_1, t_1; x_2^{(0)}, t_2^{(0)})|^2 \int_{-\infty}^{\infty} v dt_2 |\mathcal{J}_1(x_2, t_2; x_1^{(0)}, t_1^{(0)})|^2, \quad (\text{S55})$$

$$\pm 2\text{Re}[\chi(x_1^{(0)}, t_1^{(0)}; x_2^{(0)}, t_2^{(0)})], \quad (\text{S56})$$

where,

$$\chi(x_1^{(0)}, t_1^{(0)}; x_2^{(0)}, t_2^{(0)}) = \iint_{t_0}^{\infty} v^2 dt_1 dt_2 \mathcal{I}_1(x_1, t_1; x_1^{(0)}, t_1^{(0)}) \mathcal{I}_2(x_2, t_2; x_2^{(0)}, t_2^{(0)}) \mathcal{J}_2^*(x_1, t_1; x_2^{(0)}, t_2^{(0)}) \mathcal{J}_1^*(x_2, t_2; x_1^{(0)}, t_1^{(0)}). \quad (\text{S57})$$

This can be simplified further and we obtain,

$$\chi(x_1^{(0)}, t_1^{(0)}; x_2^{(0)}, t_2^{(0)}) = \int_{-\infty}^{\infty} dk |\phi(k)|^2 \mathcal{R}_k^* \mathcal{T}_k e^{ik[x_0^{(2)} - vt_0^{(2)} + x_0^{(1)} + vt_0^{(1)}]} \quad (\text{S58})$$

$$\times \int_{-\infty}^{\infty} dk' |\phi(k')|^2 \mathcal{R}_{k'}^* \mathcal{T}_{k'} e^{ik'[-x_0^{(2)} + vt_0^{(2)} - x_0^{(1)} - vt_0^{(1)}]}. \quad (\text{S59})$$

Similarly, the first two term in the expression for $P(11)_{\text{B/F}}$ can be simplified as follows,

$$\int_{-\infty}^{\infty} v dt_1 |\mathcal{I}_1(x_1, t_1; x_1^{(0)}, t_1^{(0)})|^2 = \int_{-\infty}^{\infty} \frac{v dt_1}{2\pi} \int_{-\infty}^{\infty} dk_1 e^{ik_1(x_1 - vt_1 - x_1^{(0)} + vt_1^{(0)})} \phi^*(k_1) \mathcal{T}_{k_1} \quad (\text{S60})$$

$$\times \int_{-\infty}^{\infty} dk_1' e^{-ik_1'(x_1 - vt_1 - x_1^{(0)} + vt_1^{(0)})} \phi(k_1') \mathcal{T}_{k_1'}^*, \quad (\text{S61})$$

$$= \int_{-\infty}^{\infty} dk_1 |\phi(k_1)|^2 |\mathcal{T}_{k_1}|^2. \quad (\text{S62})$$

Here, we used the fact that the integral over time give rise to $\delta(k_1 - k'_1)$. By similar set of calculations, we get, $\int_{-\infty}^{\infty} v dt_2 |\mathcal{I}_1(x_2, t_2; x_1^{(0)}, t_1^{(0)})|^2 = \int_{-\infty}^{\infty} dk_1 |\phi(k_1)|^2 |\mathcal{R}_{k_1}|^2$. Therefore, the probability $P(11)_{\text{B/F}}$ can be written as,

$$P(11)_{\text{B/F}} = \left(\int_{-\infty}^{\infty} dk |\mathcal{T}_k|^2 |\phi(k)|^2 \right)^2 + \left(\int_{-\infty}^{\infty} dk |\mathcal{R}_k|^2 |\phi(k)|^2 \right)^2, \quad (\text{S63})$$

$$\pm \chi(x_1^{(0)}, t_1^{(0)}; x_2^{(0)}, t_2^{(0)}). \quad (\text{S64})$$

We would like to understand the interference term in the probability, $P(11)_{\text{B/F}}$. The interference term is given as,

$$\chi(x_1^{(0)}, t_1^{(0)}; x_2^{(0)}, t_2^{(0)}) = \int_{-\infty}^{\infty} dk |\phi(k)|^2 \mathcal{R}_k^* \mathcal{T}_k e^{ik[x_2^{(0)} - vt_2^{(0)} + x_1^{(0)} + vt_1^{(0)}]} \quad (\text{S65})$$

$$\times \int_{-\infty}^{\infty} dk' |\phi(k')|^2 \mathcal{R}_{k'}^* \mathcal{T}_{k'} e^{ik'[-x_2^{(0)} + vt_2^{(0)} - x_1^{(0)} - vt_1^{(0)}]}, \quad (\text{S66})$$

$$= \int_{-\infty}^{\infty} dk |\phi(k)|^2 \mathcal{R}_k^* \mathcal{T}_k e^{ikx} \int_{-\infty}^{\infty} dk' |\phi(k')|^2 \mathcal{R}_{k'}^* \mathcal{T}_{k'} e^{-ik'x}, \quad (\text{S67})$$

$$= - \left| \int_{-\infty}^{\infty} dk |\phi(k)|^2 \mathcal{R}_k^* \mathcal{T}_k e^{ikx} \right|^2 \leq 0. \quad (\text{S68})$$

where $x = x_2^{(0)} - vt_2^{(0)} + x_1^{(0)} + vt_1^{(0)}$. Hence, we obtain that χ is a real function and is always negative. This tells us that the fermions always have the tendency to anti-bunch with respect to bosons, i.e., $P(11)_{\text{F}} \geq P(11)_{\text{B}}$. Since the sources are located are equal distance from the collider but on the opposite sides, Fig. 1a, then for simultaneously arriving wave packets ($t_1^{(0)} = t_2^{(0)}$) and we have $x = 0$ and we obtain $P(11)_{\text{F}}$ as shown in Fig. 2a,b. We end this subsection by evaluating the probability of the event $P(20)$ of receiving both the particles in the same detector, D_1 (or D_2). By using Eq. (S46) and Eq. (S48), we get,

$$P(20)_{\text{B/F}} = \frac{1}{2} \iint_{t_0}^{\infty} v^2 dt_1 dt_2 |\mathcal{I}_1(x_1, t_1; x_1^{(0)}, t_1^{(0)}) \mathcal{J}_2(x_2, t_2; x_2^{(0)}, t_2^{(0)}) \pm \mathcal{I}_1(x_2, t_2; x_1^{(0)}, t_1^{(0)}) \mathcal{J}_2(x_1, t_1; x_2^{(0)}, t_2^{(0)})|^2. \quad (\text{S69})$$

The factor of 1/2 comes from the fact that we have indistinguishable particles and we are integrating over the times t_1 and t_2 and both particles end up in the same detector. The probability can be written as,

$$P(20)_{\text{B/F}} = \int_{-\infty}^{\infty} v dt_1 |\mathcal{I}_1(x_1, t_1; x_1^{(0)}, t_1^{(0)})|^2 \int_{-\infty}^{\infty} v dt_2 |\mathcal{J}_2(x_2, t_2; x_1^{(0)}, t_1^{(0)})|^2, \quad (\text{S70})$$

$$\pm \text{Re}[\mathcal{G}(x_1^{(0)}, t_1^{(0)}; x_2^{(0)}, t_2^{(0)})] = P(02)_{\text{B/F}}, \quad (\text{S71})$$

where,

$$\mathcal{G}(x_1^{(0)}, t_1^{(0)}; x_2^{(0)}, t_2^{(0)}) = \iint_{t_0}^{\infty} v^2 dt_1 dt_2 \mathcal{I}_1(x_1, t_1; x_1^{(0)}, t_1^{(0)}) \mathcal{J}_2(x_2, t_2; x_2^{(0)}, t_2^{(0)}) \mathcal{J}_2^*(x_1, t_1; x_2^{(0)}, t_2^{(0)}) \mathcal{I}_1^*(x_2, t_2; x_1^{(0)}, t_1^{(0)}), \quad (\text{S72})$$

$$= -\chi(x_1^{(0)}, t_1^{(0)}; x_2^{(0)}, t_2^{(0)}). \quad (\text{S73})$$

In the case of classical waves (denoted with the subscript, ‘‘CW’’), we do not have the interference terms between direct and exchange processes and the probability with two active sources of waves is simply given as,

$$P(11)_{\text{CW}} = \int_{-\infty}^{\infty} v dt_1 |\mathcal{I}_1(x_1, t_1; x_1^{(0)}, t_1^{(0)})|^2 \int_{-\infty}^{\infty} v dt_2 |\mathcal{I}_2(x_2, t_2; x_1^{(0)}, t_1^{(0)})|^2, \quad (\text{S74})$$

$$+ \int_{-\infty}^{\infty} v dt_1 |\mathcal{J}_2(x_1, t_1; x_2^{(0)}, t_2^{(0)})|^2 \int_{-\infty}^{\infty} v dt_2 |\mathcal{J}_1(x_2, t_2; x_1^{(0)}, t_1^{(0)})|^2, \quad (\text{S75})$$

$$= \left(\int_{-\infty}^{\infty} dk |\mathcal{T}_k|^2 |\phi(k)|^2 \right)^2 + \left(\int_{-\infty}^{\infty} dk |\mathcal{R}_k|^2 |\phi(k)|^2 \right)^2, \quad (\text{S76})$$

$$P(20)_{\text{CW}} = \int_{-\infty}^{\infty} v dt_1 |\mathcal{I}_1(x_1, t_1; x_1^{(0)}, t_1^{(0)})|^2 \int_{-\infty}^{\infty} v dt_2 |\mathcal{J}_2(x_2, t_2; x_1^{(0)}, t_1^{(0)})|^2, \quad (\text{S77})$$

$$= \left(\int_{-\infty}^{\infty} dk |\mathcal{T}_k|^2 |\phi(k)|^2 \right)^2 \left(\int_{-\infty}^{\infty} dk |\mathcal{R}_k|^2 |\phi(k)|^2 \right)^2 = P(02)_{\text{CW}}. \quad (\text{S78})$$

III. TOY MODEL FOR APPARENT BUNCHING OF FERMIONS

In this section we show an apparent bunching of fermions which corresponds to the fact that the antibunching probability of fermions, $P(11)_F$ recedes that of classical particles, $P(11)_{Cl}$. In other words, we have the inequality, $P(11)_F \leq P(11)_{Cl}$ for certain values of the tunneling amplitude. This illustrates that by choosing the benchmark $\mathcal{B}_1 = P(11)_{Cl}$ doesn't not reflect the true statistical behaviour of fermions/bosons. (In the later part of the supplemental material, Sec. V, we define another benchmark \mathcal{B}_2 which will successfully determine the underlying statistics.) Consider a single particle coming in from source, S_1 . Then, it can end up in either of the two detectors, D_1 to D_2 . The diagrams, Fig. S1, shows the different trajectories for the particle to go from S_1 to D_1 or D_2 . The amplitude for different processes can be written as,

$$A_0^{(1 \rightarrow 1)} = \rho_1, \quad A_{n \neq 0}^{(1 \rightarrow 1)} = \tau_1 \tau_2 \rho_2^{2n-1} e^{in\varphi}, \quad \text{and} \quad A_{n+\frac{1}{2}}^{(1 \rightarrow 2)} = \tau_1 \tau_2 \rho_2^{2n} e^{i(n+\frac{1}{2})\varphi}. \quad (\text{S79})$$

where the subscript n refers to the winding number in the corresponding amplitude. Note that, the amplitude $A_n^{(1 \rightarrow 1)}$ comes with a phase $e^{in\varphi}$, this is the orbital phase (equivalent to kL in the section, Sec. IIB) acquired by the particle as it goes around the QAD n number of times, Fig. S1a. Similarly, when the particle goes from S_1 to D_2 , it will acquire a phase, $e^{i(n+\frac{1}{2})\varphi}$, Fig. S1b. With the single-particle amplitude written, single-particle probability in general can be written as follows,

$$\mathcal{P}(1 \rightarrow 1) = \sum_{n,m=0}^{\infty} A_n^{(1 \rightarrow 1)*} A_m^{(1 \rightarrow 1)} f(|n-m|), \quad (\text{S80})$$

where the function $f(|n-m|)$ is the decay function for $m \neq n$ and determines the contribution of different interference terms ($A_n^{(1 \rightarrow 1)*} A_m^{(1 \rightarrow 1)}$ when $m \neq n$) in the final probability and when $m = n$, we have $f(0) = 1$. For classical particles, there are no interference between any of the processes with different winding number and hence we set, $f(|n-m|) = 0$ (for $m \neq n$) and we obtain,

$$\mathcal{P}(1 \rightarrow 1)_{Cl} = \sum_{n=0}^{\infty} A_n^{(1 \rightarrow 1)*} A_n^{(1 \rightarrow 1)} = \frac{2r^2}{1+r^2}. \quad (\text{S81})$$

In the case of plane waves we have interference among all the processes and for fermions and bosons we obtain by setting $f(|n-m|) = 1$,

$$\mathcal{P}(1 \rightarrow 1)_{F/B} = \left| \frac{r e^{i\theta} [1 - e^{i\varphi - 2i\theta}]}{1 - r^2 e^{i\varphi - i2\theta}} \right|^2 = \frac{2r^2(1 - \cos \alpha)}{1 + r^4 - 2r^2 \cos \alpha}, \quad (\text{S82})$$

for all values of the tunneling amplitude, r and $\alpha = \varphi - 2\theta$ is the total geometric phase the particle gains as it goes around the QAD. Additionally, at $\varphi = 2\theta$ ($\alpha = 0$), we have resonance in system, which corresponds to the fact that $\mathcal{P}(1 \rightarrow 1) = 0$. For better clarity in understanding the system, we would like to introduce the following notation,

$$\mathcal{P}(1 \rightarrow 1) = \sum_{n,m=0}^{\infty} A_n^{(1 \rightarrow 1)*} A_m^{(1 \rightarrow 1)} f(|n-m|), \quad (\text{S83})$$

$$= \mathcal{P}(1 \rightarrow 1)_{Cl} - \Delta, \quad (\text{S84})$$

$$\text{where, } \Delta = - \sum_{n \neq m}^{\infty} A_n^{(1 \rightarrow 1)*} A_m^{(1 \rightarrow 1)} f(|n-m|). \quad (\text{S85})$$

This implies for fermions and bosons with full interference, we have $\mathcal{P}(1 \rightarrow 1)_{F/B} = 0 = \mathcal{P}(1 \rightarrow 1)_{Cl} - \Delta$ at resonance and hence,

$$\Delta = \mathcal{P}(1 \rightarrow 1)_{Cl} = \frac{2r^2}{1+r^2} \quad (\text{full interference and at resonance, } \alpha = 0), \quad (\text{S86})$$

Next, we would like to look at the case where we have partial interference in the system. This corresponds to an intermediate case where the contribution from the interference terms ($A_n^{(1 \rightarrow 1)*} A_m^{(1 \rightarrow 1)}$ for $n \neq m$) is suppressed.

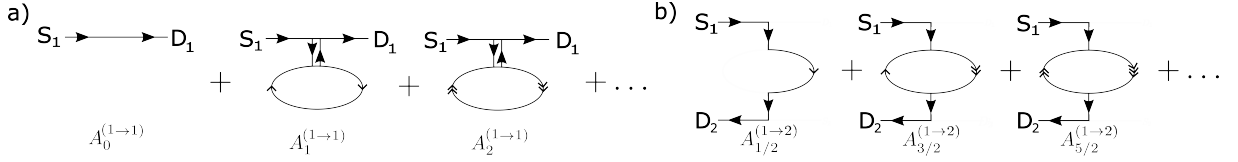


Figure S1. (a) Trajectories of the particle from the source S_1 to D_1 . The amplitude for the process $A(1 \rightarrow 1)$ is a sum of amplitudes of each of the diagram. (b) Trajectories of the particle from the source S_1 to D_2 . The amplitude for the process $A(1 \rightarrow 2)$ is a sum of amplitudes of each of the diagram. Amplitude of each of the trajectory can be written by using the junction S -matrix, Eq. (1)

Consider the simplest partial interference case, where we allow interference only among processes where the winding number differs by 1, i.e. we choose $f(|n - m|)$ as,

$$f(|n - m|) = c_1(\delta_{n,m-1} + \delta_{n,m+1}), \quad (\text{S87})$$

with $0 < c_1 \ll 1$ is the suppression factor, and the suppresses the interference of the processes where have winding number differs by 1. We neglect all the interference processes where the winding number differs by more than 1. This implies,

$$\mathcal{P}(1 \rightarrow 1)_{\text{F/B}} = \sum_{n=0}^{\infty} A_n^{(1 \rightarrow 1)*} A_n^{(1 \rightarrow 1)} + c_1 \sum_{n=0}^{\infty} A_n^{(1 \rightarrow 1)*} A_{n+1}^{(1 \rightarrow 1)} + c_1 \sum_{n=0}^{\infty} A_{n+1}^{(1 \rightarrow 1)*} A_n^{(1 \rightarrow 1)}, \quad (\text{S88})$$

$$= \mathcal{P}(1 \rightarrow 1)_{\text{Cl}} - \Delta_1, \quad (\text{S89})$$

$$\mathcal{P}(1 \rightarrow 1)_{\text{Cl}} = \frac{2r^2}{1+r^2} = \frac{2(1-t^2)}{2-t^2} \quad \text{and} \quad \Delta_1 = \frac{2c_1 r^2 (1-r^2) \cos 2\alpha}{1+r^2} = \frac{2c_1 (1-t^2) t^2 \cos 2\alpha}{2-t^2}, \quad (\text{S90})$$

with $\alpha = \frac{\varphi}{2} - \theta$ and $t^2 = 1 - r^2$. Similar set of calculation yields,

$$\mathcal{P}(1 \rightarrow 2)_{\text{F/B}} = \mathcal{P}(1 \rightarrow 2)_{\text{Cl}} + \Delta_1. \quad (\text{S91})$$

$$\mathcal{P}(1 \rightarrow 2)_{\text{Cl}} = \frac{1-r^2}{1+r^2} = \frac{t^2}{2-t^2}. \quad (\text{S92})$$

The two-particle probability, $P(11)$, where we receive one particle at each of the detector is given as,

$$P(11)_{\text{B/F}} = |A_{\text{direct}}|^2 + |A_{\text{exchange}}|^2 \pm 2\text{Re}[A_{\text{direct}}^* A_{\text{exchange}}]. \quad (\text{S93})$$

Here, A_{direct} corresponds to the processes where the particle from $S_1(S_2)$ goes to $D_1(D_2)$. Similarly, A_{exchange} refers to the processes where particle from $S_1(S_2)$ goes to $D_2(D_1)$. The corresponding amplitudes are given as,

$$A_{\text{direct}} = \sum_{n,m} A_n^{(1 \rightarrow 1)} A_m^{(2 \rightarrow 2)} = A(1 \rightarrow 1)A(2 \rightarrow 2). \quad (\text{S94})$$

$$A_{\text{exchange}} = \sum_{n,m} A_{n+\frac{1}{2}}^{(1 \rightarrow 2)} A_{m+\frac{1}{2}}^{(2 \rightarrow 1)} = A(1 \rightarrow 2)A(2 \rightarrow 1). \quad (\text{S95})$$

From here, we can simplify the probability, $P(11)_{\text{B/F}}$,

$$P(11)_{\text{B/F}} = \mathcal{P}(1 \rightarrow 1)^2 + \mathcal{P}(1 \rightarrow 2)^2 \pm 2\text{Re}[A_{\text{direct}}^* A_{\text{exchange}}]. \quad (\text{S96})$$

$$P(11)_{\text{Cl}} = \mathcal{P}(1 \rightarrow 1)_{\text{Cl}}^2 + \mathcal{P}(1 \rightarrow 2)_{\text{Cl}}^2. \quad (\text{S97})$$

The interference term in the probability, $P(11)_{\text{B/F}}$ is given as,

$$\text{Re}[A_{\text{direct}}^* A_{\text{exchange}}] = -\frac{8r^2(1-r^2)^2 \sin^2 \alpha}{(1+r^2)^2} = -\frac{8(1-t^2)t^4 \sin^2 \alpha}{(2-t^2)^2}. \quad (\text{S98})$$

We shall take the limit of small t and neglect terms of order t^4 and higher.

$$\mathcal{P}(1 \rightarrow 1)_{\text{Cl}} = 1 - \frac{t^2}{2} \quad \text{and} \quad \mathcal{P}(1 \rightarrow 2)_{\text{Cl}} = \frac{t^2}{2}. \quad (\text{S99})$$

$$\Delta_1 = c_1 t^2 \cos 2\alpha. \quad (\text{S100})$$

For evaluating $P(11)_{\text{B/F}}$, we would again work in the limit where $t \ll 1$ and keep terms only of the order (t^2),

$$\mathcal{P}(1 \rightarrow 1)^2 = \left(1 - \frac{t^2}{2} - c_1 t^2 \cos 2\alpha\right)^2 = 1 - t^2(1 + c_1 \cos 2\alpha). \quad (\text{S101})$$

$$\mathcal{P}(1 \rightarrow 2)^2 = t^4 \left(\frac{1}{2} + c_1 \cos 2\alpha\right)^2 = \mathcal{O}(t^4). \quad (\text{S102})$$

$$\text{Re}[A_{\text{direct}}^* A_{\text{exchange}}] = -\frac{8(1-t^2)t^4 \sin^2 \alpha}{(2-t^2)^2} = -2t^4 \sin^2 \alpha = \mathcal{O}(t^4). \quad (\text{S103})$$

$$\mathcal{P}(1 \rightarrow 1)_{\text{Cl}}^2 = 1 - t^2 \text{ and } \mathcal{P}(1 \rightarrow 2)_{\text{Cl}}^2 = \frac{t^4}{4} = \mathcal{O}(t^4). \quad (\text{S104})$$

From here we get the apparent bunching of fermions,

$$P(11)_{\text{B/F}} = 1 - t^2(1 + 2c_1 \cos 2\alpha) \leq 1 - t^2 = P(11)_{\text{Cl}} \text{ for } \cos 2\alpha \geq 0. \quad (\text{S105})$$

In other words, if we define the benchmark of bunching as $\mathcal{B}_1 = P(11)_{\text{Cl}}$, then we obtain,

$$\mathcal{Q}_{\text{Cl}} = P(11)_{\text{B/F}} - P(11)_{\text{Cl}} \leq 0, \quad (\text{S106})$$

for certain values of the tunneling amplitude and hence an apparent bunching of fermions. Now, we would like to pin down the processes which leads to apparent boson-like behaviour of fermions. The single particle amplitude have the following leading behaviour in t^2 ,

$$A_0^{(1 \rightarrow 1)} \sim \mathcal{O}(1), \quad A_m^{(1 \rightarrow 1)} \sim \mathcal{O}(t^2) \text{ for } m \neq 0, \quad \text{and} \quad A_{n+\frac{1}{2}}^{(1 \rightarrow 2)} \sim \mathcal{O}(t^2) \text{ for all } n. \quad (\text{S107})$$

From here we can write down the leading behaviour of all the terms in the amplitude for exchange process A_{exchange} as,

$$A_{n+\frac{1}{2}}^{(1 \rightarrow 2)} A_{m+\frac{1}{2}}^{(1 \rightarrow 2)} \sim \mathcal{O}(t^4) \in A_{\text{exchange}} \text{ for all } n, m. \quad (\text{S108})$$

Similarly, in the amplitude, A_{direct} , there are three types of terms,

$$A_0^{(1 \rightarrow 1)} A_0^{(1 \rightarrow 1)} \sim \mathcal{O}(1), \quad A_0^{(1 \rightarrow 1)} A_n^{(1 \rightarrow 1)} \sim \mathcal{O}(t^2), \quad \text{and} \quad A_m^{(1 \rightarrow 1)} A_n^{(1 \rightarrow 1)} \sim \mathcal{O}(t^4) \text{ for all } n, m \neq 0. \quad (\text{S109})$$

From here, we can say that when $t \ll 1$, the contributing terms are of the type $A_0 A_0$ and $A_0 A_n$ and it leads to apparent bunching of fermions. Similarly, in the case of non-identical junction S -matrix, Eq. (S32), if we consider interference only between the processes where winding number differs at most by 1, we get,

$$\Delta_1 = -\frac{2(1-r_1^2)(1-r_2^2)r_1 r_2 \cos(\varphi - \theta_1 - \theta_2)}{1-r_1^2 r_2^2}. \quad (\text{S110})$$

By using the same set of arguments as for the identical junctions we obtain apparent bunching of fermions for $t_1, t_2 \ll 1$.

IV. WAVE PACKET EMITTED FROM A DILUTOR QUANTUM POINT CONTACT

In this section, we calculate the wave packet shape in the case where it is emitted by a dilutor quantum point contact (QPC) in contact with the source region of the one-dimensional channel. In order to emit an electron wave packet towards the collider, we consider a source QPC at a chemical potential $\mu + eV$ and the collider leads at chemical potential $\mu = v k_f$, where k_f is the Fermi-momentum. Thus, the width of the emitted wave packet in momentum space is determined by the voltage V . The emitted wave packet is of the following form,

$$\phi(k) = \sqrt{\ell} \Theta(k - k_f) \Theta\left(k_f + \frac{eV}{v} - k\right), \quad (\text{S111})$$

where the normalization factor $\ell = \frac{v}{eV}$. The wave packet is symmetric about the mean momentum $k_0 = k_f + \frac{eV}{2v}$. A scattered wave packet is a train of wavelets separated by L , Fig. 1a. With this wave packet we would like to calculate

the overlap of two wavelets separated in winding number by $|n - m| \neq 0$,

$$f(|n - m|) = \int_{-\infty}^{\infty} dx \phi(x + |n - m|L)^* \phi(x), \quad (\text{S112})$$

$$= \frac{\ell}{2\pi} \int_{k_f}^{k_f + \frac{1}{\ell}} dk_1 dk_2 \int_{-\infty}^{\infty} dx e^{ik_1 x} e^{-ik_2 x} e^{-ik_2 |n - m|L}, \quad (\text{S113})$$

$$= \ell \int_{k_f}^{k_f + \frac{1}{\ell}} dk_1 dk_2 e^{-ik_2 |n - m|L} \delta(k_1 - k_2), \quad (\text{S114})$$

$$= \ell \int_{k_f}^{k_f + \frac{1}{\ell}} dk e^{-ikL} \frac{(-i|n - m|L)}{(-i|n - m|L)}, \quad (\text{S115})$$

$$= \frac{i\ell}{|n - m|L} \left[e^{-i(k_f + \frac{1}{\ell})|n - m|L} - e^{-ik_f |n - m|L} \right], \quad (\text{S116})$$

$$= \frac{ie^{-ik_f |n - m|L}}{|n - m|} \frac{\ell}{L} \left[e^{-i|n - m|\frac{\ell}{L}} - 1 \right], \quad (\text{S117})$$

which characterizes the suppression of interference, as detailed in the main text.

Although ℓ characterizes the decay of interference, the width of a single wave packet is strictly speaking not given by ℓ . In real space, the wave packet is given as,

$$\tilde{\phi}(x) = \frac{e^{ik_f x}}{ix} \sqrt{\frac{\ell}{2\pi}} \left[e^{ix/\ell} - 1 \right]. \quad (\text{S118})$$

However, due to the sharp Fermi surface in Eq. (S111), the function $\tilde{\phi}(x)$ decays slowly, leading to a diverging variance $\langle x^2 \rangle$. Nevertheless, in practice we do get a wave packet that have a finite width in the real space. One can understand this by considering two possible models, first, considering the QPC operating at finite temperature, $1/\beta$, and second, where the QPC is turned ON for a finite time T .

A. Wave packet in case of non-zero temperature β^{-1}

Consider a QPC at a temperature $\beta^{-1} > 0$. As result of finite temperature, the wave packet emitted by the QPC will have smearing (at the end) unlike the rectangular wave packet, Eq. (S111). The wave packet is given as follows,

$$\phi(k) = \frac{1}{\sqrt{\mathcal{N}}} \left[1 - f_F(k - k_f) \right] \left[f_F(k - k_f - \frac{eV}{v}) \right], \quad (\text{S119})$$

where \mathcal{N} is the normalization factor which in the limit $\beta \rightarrow \infty$ is equal to $\frac{v}{eV}$ and we have the Fermi function (we set $k_B = 1$ here),

$$f_F(k) = \frac{1}{e^{\beta v k} + 1}, \quad (\text{S120})$$

and $\lim_{\beta \rightarrow \infty} f_F(k) = \Theta(k)$. We would like to calculate the variance of the wave packet in the position space and therefore we begin by evaluating the wave packet in the position space,

$$\tilde{\phi}(x) = \frac{1}{\sqrt{2\pi}} \int_{-\infty}^{\infty} dk e^{ikx} \phi(k), \quad (\text{S121})$$

$$= \frac{e^{ik_f x}}{\sqrt{2\pi\mathcal{N}}} \int_{-\infty}^{\infty} dk e^{ikx} f_F(k - \frac{eV}{v}) + \frac{e^{ik_f x}}{\sqrt{2\pi\mathcal{N}}} \int_{-\infty}^{\infty} dk e^{ikx} f_F(k - \frac{eV}{v}) f_F(k), \quad (\text{S122})$$

$$= W_1 + W_2, \quad (\text{S123})$$

where \mathcal{N} is the normalization factor for the wave packet. We first evaluate W_1 as follows,

$$W_1 = \frac{e^{ik_f x}}{\sqrt{2\pi\mathcal{N}}} \int_{-\infty}^{\infty} dk e^{ikx} \frac{1}{e^{\beta v k - \beta eV} + 1}, \quad (\text{S124})$$

$$= \frac{e^{i(k_f + \frac{eV}{v})x}}{\beta v \sqrt{2\pi\mathcal{N}}} \int_{-\infty}^{\infty} dq \frac{e^{i\frac{q}{\beta v}x}}{e^q + 1}, \quad (\text{S125})$$

where we have made a substitution $q = \beta vk - \beta eV$. This integral can be performed by contour integration by noting that the Fermi function have poles on the imaginary axis. This yields,

$$W_1 = -2\pi i \frac{e^{i(k_f + \frac{eV}{v})x}}{\beta v \sqrt{2\pi\mathcal{N}}} \frac{1}{2 \sinh \frac{x\pi}{v\beta}} \Theta(x) - 2\pi i \frac{e^{i(k_f + \frac{eV}{v})x}}{\beta v \sqrt{2\pi\mathcal{N}}} \frac{1}{2 \sinh \frac{x\pi}{\beta v}} \Theta(-x), \quad (\text{S126})$$

$$= -2\pi i \frac{e^{i(k_f + \frac{eV}{v})x}}{\beta v \sqrt{2\pi\mathcal{N}}} \frac{1}{2 \sinh \frac{x\pi}{\beta v}}. \quad (\text{S127})$$

The two terms are a result of closing the contour in the lower half plane and upper half plane. Similarly,

$$W_2 = \frac{e^{ik_f x}}{\sqrt{2\pi\mathcal{N}}} \int_{-\infty}^{\infty} dk e^{ikx} \frac{1}{e^{\beta vk - \beta eV} + 1} \frac{1}{e^{\beta vk} + 1} = \frac{e^{ik_f x}}{\beta v \sqrt{2\pi\mathcal{N}}} \int_{-\infty}^{\infty} dq e^{i\frac{q}{\beta v} x} \frac{1}{e^{q - \beta eV} + 1} \frac{1}{e^q + 1}, \quad (\text{S128})$$

$$= \frac{\Theta(x) e^{ik_f x}}{\beta v \sqrt{2\pi\mathcal{N}}} 2\pi i \sum_{n=0}^{\infty} \lim_{q \rightarrow eV\beta + i(2n+1)\pi} e^{i\frac{q}{\beta v} x} \frac{1}{e^q + 1} \frac{q - \beta eV - i(2n+1)\pi}{e^{q - \beta eV} + 1} \quad (\text{S129})$$

$$- \frac{\Theta(-x) e^{ik_f x}}{\beta v \sqrt{2\pi\mathcal{N}}} 2\pi i \sum_{n=0}^{\infty} \lim_{q \rightarrow eV\beta - i(2n+1)\pi} e^{i\frac{q}{\beta v} x} \frac{1}{e^q + 1} \frac{q + \beta eV + i(2n+1)\pi}{e^{q - \beta eV} + 1} \quad (\text{S130})$$

$$+ \frac{\Theta(x) e^{ik_f x}}{\beta v \sqrt{2\pi\mathcal{N}}} 2\pi i \sum_{n=0}^{\infty} \lim_{q \rightarrow i(2n+1)\pi} e^{i\frac{q}{\beta v} x} \frac{1}{e^{q - \beta eV} + 1} \frac{q - i(2n+1)\pi}{e^q + 1} \quad (\text{S131})$$

$$- \frac{\Theta(-x) e^{ik_f x}}{\beta v \sqrt{2\pi\mathcal{N}}} 2\pi i \sum_{n=0}^{\infty} \lim_{q \rightarrow -i(2n+1)\pi} e^{i\frac{q}{\beta v} x} \frac{1}{e^{q - \beta eV} + 1} \frac{q + i(2n+1)\pi}{e^q + 1}. \quad (\text{S132})$$

We have four contributions, coming from contour integration with poles on the imaginary axis (lower and upper half plane). We obtain,

$$W_2 = -\frac{2\pi i}{\beta v \sqrt{2\pi\mathcal{N}}} \frac{e^{i(\frac{eV}{v} + k_f)x}}{1 - e^{\beta eV}} \frac{1}{2 \sinh \frac{x\pi}{\beta v}} - \frac{2\pi i}{\beta v \sqrt{2\pi\mathcal{N}}} \frac{e^{ik_f x}}{1 - e^{-\beta eV}} \frac{1}{2 \sinh \frac{x\pi}{\beta v}}. \quad (\text{S133})$$

Compiling all the results we get the following,

$$\tilde{\phi}(x) = W_1 + W_2 = \frac{1}{\sqrt{2\pi\mathcal{N}}} \int_{-\infty}^{\infty} dk e^{ikx} f_F(k - \frac{eV}{v}) - \int_{-\infty}^{\infty} dk e^{ikx} f_F(k - \frac{eV}{v}) f(k), \quad (\text{S134})$$

$$= -2\pi i \frac{e^{i(\frac{eV}{v} + k_f)x}}{\beta v \sqrt{2\pi\mathcal{N}}} \frac{1}{2 \sinh \frac{x\pi}{\beta v}} + \frac{2\pi i}{\beta \sqrt{\mathcal{N}}} \frac{e^{i(\frac{eV}{v} + k_f)x}}{1 - e^{eV\beta v}} \frac{1}{2 \sinh \frac{x\pi}{\beta v}} + \frac{2\pi i}{\beta v \sqrt{\mathcal{N}}} \frac{e^{ik_f x}}{1 - e^{-eV\beta}} \frac{1}{2 \sinh \frac{x\pi}{\beta v}}, \quad (\text{S135})$$

$$= \frac{\pi i}{\beta v \sqrt{2\pi\mathcal{N}}} \frac{e^{ik_f x}}{1 - e^{-eV\beta}} \frac{1}{\sinh \frac{x\pi}{\beta v}} \left[1 - e^{i\frac{eV}{v}x} \right]. \quad (\text{S136})$$

When $\beta eV \gg 1$, we recover Eq. (S118):

$$\tilde{\phi}(x) = -\frac{\pi i e^{ik_f x}}{\beta v \sqrt{2\pi\mathcal{N}}} \frac{\beta v}{x\pi} \left[e^{i\frac{eV}{v}x} - 1 \right] = \frac{e^{ik_f x}}{ix} \sqrt{\frac{\ell}{2\pi}} \left[e^{i\frac{eV}{v}x} - 1 \right]. \quad (\text{S137})$$

Let us calculate the expectation value of x^2 ,

$$\langle \hat{x}^2 \rangle = \int_{-\infty}^{\infty} dx x^2 |\tilde{\phi}(x)|^2, \quad (\text{S138})$$

$$= \frac{4\pi^2}{\beta^2 v^2 \mathcal{N} \left(1 - e^{-eV\beta} \right)^2} \int_{-\infty}^{\infty} dx x^2 \frac{\sin^2 \frac{eV}{2v} x}{\sinh^2 \frac{x\pi}{\beta v}}, \quad (\text{S139})$$

$$= \frac{4\pi^2}{\beta^2 v^2 \mathcal{N} \left(1 - e^{-eV\beta} \right)^2} \left(\frac{2v}{eV} \right)^3 \frac{\pi^2 \left(\frac{2\pi}{eV\beta} + 3 \left(\frac{2\pi}{eV\beta} - \pi \coth \frac{eV\beta}{2} \right) \sinh^{-2} \frac{eV\beta}{2} \right)}{6 \left(\frac{2\pi}{eV\beta} \right)^4}. \quad (\text{S140})$$

In the case when $\frac{\beta v}{\ell} \gg 1$ (and thus $\beta eV \gg 1$) we get the following simplifications,

$$\langle \hat{x}^2 \rangle \approx \frac{4\pi^2}{\beta^2 v^2 \mathcal{N}} \left(\frac{2v}{eV} \right)^3 \frac{\pi^2}{6} \left(\frac{eV\beta}{2\pi} \right)^3 = \frac{2\pi\beta v}{3\mathcal{N}} = \frac{2\pi\beta v^2}{3eV} = \frac{2\pi\beta v\ell}{3}. \quad (\text{S141})$$

with $\mathcal{N} \approx \frac{eV}{v} = \frac{1}{\ell}$ (for $\beta eV \gg 1$) and note that we have $\langle x \rangle = 0$. Therefore the wave packet width in position space is $\Delta x = \sqrt{\langle x^2 \rangle - \langle x \rangle^2} \approx \sqrt{\frac{2\pi\beta v\ell}{3}}$.

B. Wave packet in case of finite operating window T of the QPC

In a real experimental setup when the source is turned ON for a duration T , then the maximum spread of the wave packet is restricted by vT , where v being the velocity of the wave packet. We consider the following wave packet,

$$\phi(x) = \begin{cases} \frac{e^{ik_f x}}{ix} \sqrt{\frac{\ell}{2\pi\mathcal{N}}} [e^{ix/\ell} - 1] & \text{for } |x| \leq \frac{vT}{2} \\ 0 & \text{for } |x| > \frac{vT}{2} \end{cases} \quad (\text{S142})$$

where \mathcal{N} is the normalization of the wave packet in the position space. If the duration for which the source is turned ON is sufficiently large then in that case normalization is unchanged and we have $\mathcal{N} = 1$. Using this wave packet we are going to calculate the variance. This is evaluated as follows,

$$\langle x^2 \rangle = \int_{-\frac{vT}{2}}^{\frac{vT}{2}} dx x^2 \frac{\ell}{2\pi\mathcal{N}x^2} \left[2 - 2 \cos\left(\frac{x}{\ell}\right) \right], \quad (\text{S143})$$

$$= \frac{\ell}{\pi} \left(vT - 2\ell \sin\left(\frac{vT}{2\ell}\right) \right). \quad (\text{S144})$$

In the limit where $\frac{vT}{2\ell} \gg 1$, we have $\mathcal{N} \rightarrow 1$ because $|\phi(x)|^2$ falls as x^{-2} and therefore the normalization of the wave packet doesn't change and we have $\mathcal{N} \rightarrow 1$. This implies,

$$\langle x^2 \rangle \approx \sqrt{\frac{\ell v T}{\pi}}. \quad (\text{S145})$$

From here obtain,

$$\frac{\sqrt{\langle x^2 \rangle}}{vT} = \sqrt{\frac{\ell}{\pi v T}} \ll 1. \quad (\text{S146})$$

hence, the spatial size of the wave packet is much smaller than vT as one would expect.

V. BENCHMARK FOR EXTRACTING THE TRUE MUTUAL STATISTICS OF PARTICLES

In this section we are going to extract the quantum statistics of the colliding particles by defining the benchmark, \mathcal{B}_2 . Outcome of the two-particle processes is affected by the underlying statistics of the particles and by choosing the correct observable we can extract the statistical information. Probabilities of different single particle events are independent of statistics because of the absence of any statistical interactions due to other particles. Statistics of the underlying particles affects all processes where we have at least two particles in the collider. However, due to the non-point-like geometry we find that there are infinite number of possible trajectories for any single particle event, Fig. S1a-b, and self interference of such trajectories leads to the apparent bunching of fermions as we discussed in the main text and Sec. III. Therefore in order to extract the true information about the mutual statistics we define, \mathcal{Q}_{Irr} ,

$$\mathcal{Q}_{\text{Irr}} = P(11)_{s_1 s_2} - \mathcal{P}(1 \rightarrow 1)_{s_1} \mathcal{P}(2 \rightarrow 2)_{s_2} - \mathcal{P}(1 \rightarrow 2)_{s_1} \mathcal{P}(2 \rightarrow 1)_{s_2} = P(11)_{s_1 s_2} - \mathcal{B}_2, \quad (\text{S147})$$

where $\mathcal{B}_2 = \mathcal{P}(1 \rightarrow 1)_{s_1} \mathcal{P}(2 \rightarrow 2)_{s_2} + \mathcal{P}(1 \rightarrow 2)_{s_1} \mathcal{P}(2 \rightarrow 1)_{s_2}$ and $P(11)_{s_1 s_2}$ refers to the probability when each of the detector receives one particle with both the sources S_1 and S_2 active (subscripts denote the active sources). The single particle probability $\mathcal{P}(1 \rightarrow 1)_{s_1}$ and $\mathcal{P}(1 \rightarrow 2)_{s_1}$ corresponds to the case where we have only single active source

	Distinguishable particle(s)		Indistinguishable particle(s)	
	Classical particle(s)	Classical wave(s)	Quantum particle(s)	Quantum wave(s)
One active source (S_1)	$\mathcal{P}(1 \rightarrow 1)_{S_1} = \sum_{n=0}^{\infty} A_n^{(1 \rightarrow 1)} ^2$ $\mathcal{P}(1 \rightarrow 2)_{S_1} = \sum_{n=0}^{\infty} A_{n+\frac{1}{2}}^{(1 \rightarrow 2)} ^2$	$\mathcal{P}(1 \rightarrow 1)_{S_1} = \sum_{n=0}^{\infty} A_n^{(1 \rightarrow 1)} ^2$ $\mathcal{P}(1 \rightarrow 2)_{S_1} = \sum_{n=0}^{\infty} A_{n+\frac{1}{2}}^{(1 \rightarrow 2)} ^2$	$\mathcal{P}(1 \rightarrow 1)_{S_1} = \sum_{n=0}^{\infty} A_n^{(1 \rightarrow 1)} ^2$ $\mathcal{P}(1 \rightarrow 2)_{S_1} = \sum_{n=0}^{\infty} A_{n+\frac{1}{2}}^{(1 \rightarrow 2)} ^2$	$\mathcal{P}(1 \rightarrow 1)_{S_1} = \sum_{n=0}^{\infty} A_n^{(1 \rightarrow 1)} ^2$ $\mathcal{P}(1 \rightarrow 2)_{S_1} = \sum_{n=0}^{\infty} A_{n+\frac{1}{2}}^{(1 \rightarrow 2)} ^2$
Two active sources (S_1 and S_2)	$P(11) = \mathcal{P}(1 \rightarrow 1)_{S_1} \mathcal{P}(2 \rightarrow 2)_{S_2}$ $+ \mathcal{P}(1 \rightarrow 2)_{S_1} \mathcal{P}(2 \rightarrow 1)_{S_2}$	$P(11) = \mathcal{P}(1 \rightarrow 1)_{S_1} \mathcal{P}(2 \rightarrow 2)_{S_2}$ $+ \mathcal{P}(1 \rightarrow 2)_{S_1} \mathcal{P}(2 \rightarrow 1)_{S_2}$	$P(11) = \sum_{n,m=0}^{\infty} A_n^{(1 \rightarrow 1)} A_m^{(2 \rightarrow 2)} \pm A_{n+\frac{1}{2}}^{(1 \rightarrow 2)} A_{m+\frac{1}{2}}^{(2 \rightarrow 1)} ^2$ $\approx \mathcal{P}(1 \rightarrow 1)_{S_1} \mathcal{P}(2 \rightarrow 2)_{S_2}$ $+ \mathcal{P}(1 \rightarrow 2)_{S_1} \mathcal{P}(2 \rightarrow 1)_{S_2}$	$P(11)_{B/F} = \mathcal{P}(1 \rightarrow 1)_{S_1} \mathcal{P}(2 \rightarrow 2)_{S_2}$ $+ \mathcal{P}(1 \rightarrow 2)_{S_1} \mathcal{P}(2 \rightarrow 1)_{S_2}$ $\pm 2\text{Re} \left[\sum_{n,m,i,j=0}^{\infty} A_n^{(1 \rightarrow 1)} A_m^{(2 \rightarrow 2)} \times A_{i+\frac{1}{2}}^{(1 \rightarrow 2)*} A_{j+\frac{1}{2}}^{(2 \rightarrow 1)*} \right]$
Comment on the two benchmarks of bunching	$\mathcal{Q}_{Cl} = 0$ for all r $\mathcal{Q}_{Irr} = 0$ for all r	$\mathcal{Q}_{Cl} \leq 0$ for some r $\mathcal{Q}_{Irr} = 0$ for all r	$\mathcal{Q}_{Cl} = 0$ for all r $\mathcal{Q}_{Irr} = 0$ for all r	$\mathcal{Q}_{Cl;B/F} \leq 0$ for some r $\mathcal{Q}_{Irr;B} \leq 0$ for all r $\mathcal{Q}_{Irr;F} \geq 0$ for all r

Table I. Probabilities of different events in the extended collider with classical particles, classical waves, quantum particles and quantum waves with one or two active sources. Differences between them arises from the degree of interference they have, with classical particles there is no interference at all and with quantum waves, we have full interference (everything interferes with everything else). In the table, by quantum particles, we mean a wave packet that is localized to a region smaller than the size of the quantum anti-dot (L), which leads to less interference and therefore the probability is similar to that of classical particles. In the limit of very small width ($\ell \ll L$) we recover the classical particles probability. For extracting the statistical differences we have found that there are two benchmarks. In one, we calculate the probability, $P(11)$ and compare it with the corresponding quantity for classical particles, which doesn't remove the single particle self-interference terms and the other involves defining an irreducible part of $P(11)$ which removes the contributions from single particle interference. If we choose the first benchmark of bunching, the corresponding probability of classical particles, $P(11)_{Cl}$ and define, $\mathcal{Q}_{Cl} = P(11) - P(11)_{Cl}$, Eq. (S106). Then, we get an apparent bunching of fermions, $\mathcal{Q}_{Cl;F} \leq 0$ for certain values of r , Fig. 2a. With the second benchmark, we define the irreducible correlator, $\mathcal{Q}_{Irr} = P(11)_{S_1 S_2} - \mathcal{P}(1 \rightarrow 1)_{S_1} \mathcal{P}(2 \rightarrow 2)_{S_2} - \mathcal{P}(1 \rightarrow 2)_{S_1} \mathcal{P}(2 \rightarrow 1)_{S_2}$, Eq. (S147), one can differentiate bosons ($\mathcal{Q}_{Irr} \leq 0$) from fermions ($\mathcal{Q}_{Irr} \geq 0$) for all values of r .

S_1 . The subscript ‘‘Irr’’ means irreducible as we subtract the single-particle contributions from $P(11)$. By defining \mathcal{Q}_{Irr} in this way we extract the terms which are only sensitive to the exchange of particles and therefore have the information of the quantum statistics. For classical particles we obtain,

$$\mathcal{Q}_{Irr;Cl} = P(11)_{S_1 S_2} - \mathcal{P}(1 \rightarrow 1)_{S_1} \mathcal{P}(2 \rightarrow 2)_{S_2} - \mathcal{P}(1 \rightarrow 2)_{S_1} \mathcal{P}(2 \rightarrow 1)_{S_2}, \quad (S148)$$

$$= \mathcal{P}(1 \rightarrow 1)_{S_1} \mathcal{P}(2 \rightarrow 2)_{S_2} + \mathcal{P}(1 \rightarrow 2)_{S_1} \mathcal{P}(2 \rightarrow 1)_{S_2} \quad (S149)$$

$$- \mathcal{P}(1 \rightarrow 1)_{S_1} \mathcal{P}(2 \rightarrow 2)_{S_2} - \mathcal{P}(1 \rightarrow 2)_{S_1} \mathcal{P}(2 \rightarrow 1)_{S_2}, \quad (S150)$$

$$= 0, \quad (S151)$$

as expected because classical particles doesn't have any quantum statistics. With bosons and fermions, we have,

$$P(11)_{S_1 S_2} = |A_{\text{direct}}|^2 + |A_{\text{exchange}}|^2 \pm 2\text{Re}[A_{\text{direct}}^* A_{\text{exchange}}], \quad (S152)$$

where the $+/-$ sign corresponds to bosons/fermions. The contribution of the direct processes and the exchange processes can be simplified as follows using Eq. (S94),

$$A_{\text{direct}} = A(1 \rightarrow 1)A(2 \rightarrow 2) \quad \text{and} \quad A_{\text{exchange}} = A(1 \rightarrow 2)A(2 \rightarrow 1), \quad (S153)$$

$$|A_{\text{direct}}|^2 = \mathcal{P}(1 \rightarrow 1)_{S_1} \mathcal{P}(2 \rightarrow 2)_{S_2} \quad \text{and} \quad |A_{\text{exchange}}|^2 = \mathcal{P}(1 \rightarrow 2)_{S_1} \mathcal{P}(2 \rightarrow 1)_{S_2}. \quad (S154)$$

Therefore, we find that the benchmark $\mathcal{B}_2 = \mathcal{P}(1 \rightarrow 1)_{S_1} \mathcal{P}(2 \rightarrow 2)_{S_2} + \mathcal{P}(1 \rightarrow 2)_{S_1} \mathcal{P}(2 \rightarrow 1)_{S_2}$ removes all the single-particle self-interference terms and hence we have,

$$\mathcal{Q}_{Irr;B/F} = \pm 2\text{Re}[A_{\text{direct}}^* A_{\text{exchange}}]. \quad (S155)$$

The function \mathcal{Q}_{Irr} gives us the information about the statistics of the particles. It comes with specific signature for bosons and fermions and hence distinguishes the statistical nature of bosons and fermions. The earlier defined \mathcal{Q}_{Cl} didn't remove the self interference contributions to the probability $P(11)_{F/B}$ and hence was giving false information about the statistics of the colliding particles. We emphasize that \mathcal{Q}_{Cl} , Eq. (S106) is *not* the correct benchmark to extract the mutual statistics of particles. We summarize the results for the probabilities for classical particles, classical waves, quantum particles and quantum waves with single active source and two active sources in the table, Tab. V. Quantum particles mentioned here refers to the narrow wave packets of indistinguishable particles. Width of the wave packet controls the degree of the interference in the system. With extremely narrow wave packet ($\sqrt{\beta v \ell} / L \ll 1$),

Eq. (S141), there is no interference at all and we recover the classical particle results. In the proposed model of the extended collider, for quantum particles (narrow wave packets), we have,

$$P(11)_{\text{B/F}} = \sum_{n,m=0}^{\infty} |A_n^{(1\rightarrow 1)} A_m^{(2\rightarrow 2)} \pm A_{n+\frac{1}{2}}^{(1\rightarrow 1)} A_{m+\frac{1}{2}}^{(2\rightarrow 2)}|^2, \quad (\text{S156})$$

$$= \sum_{n=0}^{\infty} |A_n^{(1\rightarrow 1)}|^2 \sum_{m=0}^{\infty} |A_m^{(2\rightarrow 2)}|^2 + \sum_{n=0}^{\infty} |A_{n+\frac{1}{2}}^{(1\rightarrow 2)}|^2 \sum_{m=0}^{\infty} |A_{m+\frac{1}{2}}^{(2\rightarrow 1)}|^2 \pm 2\text{Re} \left[A_n^{(1\rightarrow 1)} A_{n+\frac{1}{2}}^{(1\rightarrow 2)} A_m^{(2\rightarrow 2)} A_{m+\frac{1}{2}}^{(2\rightarrow 1)} \right], \quad (\text{S157})$$

$$\approx \sum_{n=0}^{\infty} |A_n^{(1\rightarrow 1)}|^2 \sum_{m=0}^{\infty} |A_m^{(2\rightarrow 2)}|^2 + \sum_{n=0}^{\infty} |A_{n+\frac{1}{2}}^{(1\rightarrow 2)}|^2 \sum_{m=0}^{\infty} |A_{m+\frac{1}{2}}^{(2\rightarrow 1)}|^2. \quad (\text{S158})$$

With narrow wave packets ($\sqrt{\beta v \ell}/L \ll 1$), Eq. (S141), we are going to have,

$$A_n^{(1\rightarrow 1)} A_{n+\frac{1}{2}}^{(1\rightarrow 2)} \rightarrow 0, \quad (\text{S159})$$

which can be understood from the fact that a wave packet from S_1 going to D_2 will have to travel an extra distance of half the loop size ($L/2$), and with narrow wave packet, its interference with wave packet from S_1 to D_1 is very small and can be neglected. Therefore, the differences that we see in the probabilities is a result of difference in the level of interference. The level of interference can be varied by changing the spatial width of the wave packet.

VI. ESTIMATION OF SPATIAL WIDTH OF THE SCATTERED WAVE PACKET AND THE CONDITION ON THE EMISSION RATE AT THE SOURCES

An incoming wave packet after scattering, becomes an infinite series of wavelets in the transmission/reflection lead, Fig. 1a. The center of each of the wavelet is separated by L . Since, our calculations requires no interference between wave packets from the same source, we would like to calculate the spatial width of the transmitted/reflected wave packets and then determine the correct emission rate of the sources. In the following we present an approximate calculation of the width of the scattered wave packet. By using Eq. (2) and Eq. (3), we have,

$$\tilde{\phi}_{d_1}(x) = \rho_1 \tilde{\phi}_{s_1}(x) + \rho_2 \tau_1 \tau_2 \tilde{\phi}_{s_1}(x+L) + \rho_2^3 \tau_1 \tau_2 \tilde{\phi}_{s_1}(x+2L) + \dots. \quad (\text{S160})$$

For calculating the variance of the transmitted wave packet, we first need to evaluate the expectation value of the position operator, \hat{x} and \hat{x}^2 ,

$$\langle \hat{x} \rangle = \int_{-\infty}^{\infty} dx x |\tilde{\phi}_{d_1}(x)|^2 \quad \text{and} \quad \langle \hat{x}^2 \rangle = \int_{-\infty}^{\infty} dx x^2 |\tilde{\phi}_{d_1}(x)|^2. \quad (\text{S161})$$

Since, the transmitted wave packet have infinite number of terms, Eq. (S160), calculation of the expectations value becomes non-trivial and therefore we do the calculations in the classical limit [48] and drop all the cross terms. By only considering the classical contribution to the expectation values, we obtain for the transmitted wave packet,

$$\langle \hat{x} \rangle_{\text{trans}} = |\rho_1|^2 \int_{-\infty}^{\infty} dx |\tilde{\phi}_{s_1}(x)|^2 x + |\rho_2 \tau_1 \tau_2|^2 \int_{-\infty}^{\infty} dx |\tilde{\phi}_{s_1}(x+L)|^2 x + \dots, \quad (\text{S162})$$

$$\langle \hat{x}^2 \rangle_{\text{trans}} = |\rho_1|^2 \int_{-\infty}^{\infty} dx |\tilde{\phi}_{s_1}(x)|^2 x^2 + |\rho_2 \tau_1 \tau_2|^2 \int_{-\infty}^{\infty} dx |\tilde{\phi}_{s_1}(x+L)|^2 x^2 + \dots, \quad (\text{S163})$$

where the subscript ‘‘trans’’ refers to the transmitted wave packet. Each of the term corresponds to diagram in the Fig. S1a. In the above, $\tilde{\phi}(x)$ is given by Eq. (S122). Note that the quantity $|\phi(x)|^2$ is symmetric around $x=0$ (even function) and therefore we have,

$$\int_{-\infty}^{\infty} dx |\tilde{\phi}_{s_1}(x+L)|^2 x = \int_{-\infty}^{\infty} dx |\tilde{\phi}_{s_1}(x)|^2 (x-L), \quad (\text{S164})$$

$$= L \int_{-\infty}^{\infty} dx |\tilde{\phi}_{s_1}(x)|^2 = -L. \quad (\text{S165})$$

Similarly, we have,

$$\int_{-\infty}^{\infty} dx |\tilde{\phi}_{s_1}(x+L)|^2 x^2 = \int_{-\infty}^{\infty} dx |\tilde{\phi}_{s_1}(x)|^2 (x-L)^2, \quad (\text{S166})$$

$$= L^2 \int_{-\infty}^{\infty} dx |\tilde{\phi}_{s_1}(x)|^2 + \int_{-\infty}^{\infty} dx |\tilde{\phi}_{s_1}(x)|^2 x^2 \approx L^2 + \frac{2\pi\beta v\ell}{3}, \quad (\text{S167})$$

where we have used the fact that $\int_{-\infty}^{\infty} dx |\tilde{\phi}_{s_1}(x)|^2 x^2 = \frac{2\pi\beta v\ell}{3}$, Eq. (S141), which is valid in the limit $\frac{\beta v}{\ell} \gg 1$. From here we obtain the following,

$$\langle \hat{x} \rangle_{\text{trans}} = -\frac{LR}{1+R^2} \quad \text{and} \quad \langle \hat{x}^2 \rangle_{\text{trans}} = \frac{2\pi\beta v\ell}{3} \mathcal{P}(1 \rightarrow 1)_{\text{Cl}} + \frac{L^2 R(1+R^2)}{(1-R)(1+R)^3}, \quad (\text{S168})$$

where we have $R = |\rho_1|^2 = |\rho_2|^2$. A similar set of calculations can be done for the reflected wave packet. Below, we present the spatial width of the wave packet in the limit $\sqrt{\beta v\ell}/L \ll 1$,

$$L_{\text{trans}} = \sqrt{\langle \hat{x}^2 \rangle_{\text{trans}} - \langle \hat{x} \rangle_{\text{trans}}^2} \approx \sqrt{\frac{L^2 R(R^3 + 2R^2 + 1)}{(1-R)(1+R)^4}} = \sqrt{\frac{\tau_0 v L R (R^3 + 2R^2 + 1)}{(1+R)^3}}, \quad (\text{S169})$$

$$L_{\text{refl}} = \sqrt{\langle \hat{x}^2 \rangle_{\text{refl}} - \langle \hat{x} \rangle_{\text{refl}}^2} \approx \sqrt{\frac{L^2 R(1+R^4 + 4R^2 + 2R)}{2(1-R)(1+R)^4}} = \sqrt{\frac{\tau_0 v L R (1+R^4 + 4R^2 + 2R)}{2(1+R)^3}}, \quad (\text{S170})$$

where we have τ_0 is the lifetime of the particle in the QAD. Lifetime is defined as the average time that the particle spends inside the QAD before it escapes. Lets say we created a particle inside the QAD, probability of performing one winding before escaping is R^2 , probability of performing two winding before escaping is R^4 and so on. The corresponding time spent on the QAD is L/v for performing one winding and $2L/v$ for performing two winding and so on. This implies the lifetime of the particle is given as

$$\tau_0 = \frac{1}{N} \left[\frac{R^2 L}{v} + \frac{2R^4 L}{v} + \frac{3R^6 L}{v} + \dots \right] = \frac{L}{v(1-R^2)}, \quad (\text{S171})$$

where N is the normalization factor and is equal to the expectation value of 1 with respect to the probability of escaping after performing n number of winding, i.e. $N = \sum_{n=1}^{\infty} R^{2n}$. We again emphasize that the calculations presented in this section are in the limit when the wave packets are well localized, $\frac{\sqrt{\beta v\ell}}{L} \ll 1$.

Since we have assumed that the emission rate at the sources is λ , this implies that the average time difference between the emission of consecutive particles is $\frac{1}{\lambda}$. Note that our analysis presented here assumes no more than two particles simultaneously in the collider and this can be achieved when we have the average distance between the particles is much larger than the width of the scattered wave packet ($\sim L$ see Eq. (S169) and Eq. (S170)), i.e. $\frac{v}{\lambda} \gg L$. This is the condition on λ as mentioned in the main text.

A. Comment on the case with many particles emitted from the source

Here, we would like to see the case where we have multiple particles simultaneously in the collider emitted from the source(s). We begin by estimating the probability having two particles within the time interval $\epsilon \sim \frac{L}{v}$ given the source, say S_1 emitted n number of particles. So, the probability of having two particles within the time interval ϵ with emission of n number particle, $P_n^{(2)}$,

$$P_n^{(2)} = \binom{n}{2} \frac{\epsilon(2T - \epsilon)}{T^2}, \quad (\text{S172})$$

$$= \frac{n(n-1)}{2} \frac{(2T\epsilon - \epsilon^2)}{T^2}. \quad (\text{S173})$$

where $\epsilon(2T - \epsilon)$ corresponds to the area of the strip in the phase space where the particles are within time interval ϵ . Lets assume that ϵ is small compared to T and therefore we can neglect ϵ^2 terms,

$$P_n^{(2)} = \frac{\epsilon}{T} n(n-1). \quad (\text{S174})$$

In the case where we have lots of particles emitted from the source in a given time interval T , we can approximate the above calculated probability as follows,

$$P_n^{(2)} \approx \frac{\epsilon}{T} \lambda^2 T^2 = \epsilon \lambda^2 T, \quad (\text{S175})$$

where we have used the fact that on average we have $n = \lambda T$ number of particles from the source(s). Generalizing this formula to find the probability of having three particles within the time interval ϵ is given as,

$$P_n^{(3)} \approx \frac{\epsilon^2 T n^3}{T^3} = \epsilon^2 \lambda^3 T. \quad (\text{S176})$$

From the above calculations, we can see the probability of having more and more particles within a time interval is suppressed by $\epsilon \lambda$. So, in our case we choose a low enough emission rate ($\lambda \ll \frac{v}{L}$) and therefore the undesired multi-particle interference effects are small and can be ignored.

VII. RELATION BETWEEN THE CURRENT-CURRENT CORRELATIONS AND PROBABILITIES

In this section we are going to look at the antibunching probability $P(11)_{\text{F/B}}$ of receiving one particle at each detector D_1 and D_2 with particles coming in from both the sources. We establish the relationship between the two-particle probability $P(11)_{\text{F/B}}$ and the cross-current correlations function measured at the detectors, D_1 and D_2 . This is an experimentally accessible quantity. In our system, current at the detector is proportional to the number density at the detector and is given as $I_{d_i}(t_i) = e v n_{d_i}(t_i)$ for $i = 1, 2$ and e is the charge and $n_{d_i}(x, t) = \phi_{d_i}^\dagger(x, t) \phi_{d_i}(x, t)$ is the number density in terms of the field operator $\phi_{d_i}^\dagger(x, t)$. Let us begin by considering the case where we have just a single active source and we try to compute the single particle probability $\mathcal{P}(1 \rightarrow 1)$. Let us assume that the source S_1 is turned ON for the time interval $[-T/2, T/2]$ and in the calculations we $T \rightarrow \infty$. Lets say that the detector, D_1 is at the coordinate x_1 and the measurement time is t_1 . Now the incoming state is mixed state from the source S_1 and is given as,

$$\rho_{s_1} = \sum_{n_1=0}^{\infty} P_\lambda(n_1) \left[\prod_{i_1=1}^{n_1} \tilde{\phi}_{s_1}^\dagger(x_1^{(0)}, t_{i_1}^{(0)}) |\Omega\rangle \langle \Omega| \tilde{\phi}_{s_1}(x_1^{(0)}, t_{i_1}^{(0)}) \right], \quad (\text{S177})$$

where we have assumed that the emitted particles follow a Poisson distribution with emission rate λ . The probability of emitting n number of particles from the source is given as,

$$P_\lambda(n) = \frac{e^{-\lambda T} (\lambda T)^n}{n!}. \quad (\text{S178})$$

For concreteness let us consider a particular where the incoming state have n_1 number of particles from the source S_1 and using this we will calculate the number density at the detector D_1 . The state with n_1 number of particles is given as,

$$|\psi_{n_1}\rangle_{s_1} = \prod_{i_1=1}^{n_1} \tilde{\phi}_{s_1}^\dagger(x_1^{(0)}, t_{i_1}^{(0)}) |\Omega\rangle. \quad (\text{S179})$$

Number density evaluated at the detector D_1 at time t_1 is as follows,

$$\langle \psi_{n_1} | n_{d_1}(t_1) | \psi_{n_1} \rangle_{n_1} = \left| \sum_{i_1=1}^{n_1} \mathcal{I}_1(x_1, t_1; x_1^{(0)}, t_{i_1}^{(0)}) \right|^2, \quad (\text{S180})$$

where the subscript n_1 outside the angular bracket emphasizes that we work with a particular state, $|\psi_{n_1}\rangle_{s_1}$. For a dilute stochastic beam of particles we are going to have emission times well separated (mean separation being $1/\lambda$), therefore we can integrate over the emission times and obtain,

$$v \int_{-T/2}^{T/2} \prod_{i_1=1}^{n_1} dt_{i_1} \langle \psi_{n_1} | n_{d_1}(t_1) | \psi_{n_1} \rangle_{s_1} = T^{n_1-1} n_1 \mathcal{P}(1 \rightarrow 1), \quad (\text{S181})$$

$$\frac{v}{T^{n_1}} \int_{-T/2}^{T/2} \prod_{i_1=1}^{n_1} dt_{i_1} \langle \psi_{n_1} | n_{d_1}(t_1) | \psi_{n_1} \rangle_{s_1} = \frac{n_1}{T} \mathcal{P}(1 \rightarrow 1). \quad (\text{S182})$$

Averaging over number of particles from the source S_1 we have,

$$\sum_{n_1=0}^{\infty} P_{\lambda}(n_1) \frac{v}{T^{n_1}} \int_{-T/2}^{T/2} \prod_{i_1=1}^{n_1} dt_{i_1} \langle \psi_{n_1} | n_{d_1}(t_1) | \psi_{n_1} \rangle_{s_1} = \sum_{n_1=0}^{\infty} P_{\lambda}(n_1) \frac{n_1}{T} \mathcal{P}(1 \rightarrow 1), \quad (\text{S183})$$

$$= \lambda \mathcal{P}(1 \rightarrow 1). \quad (\text{S184})$$

This implies that the average current at the drain with a single active source (S_1) is given as,

$$\langle I_{d_1}(t_1) \rangle_{s_1} = e\lambda \mathcal{P}(1 \rightarrow 1), \quad (\text{a constant current in the drain } D_1) \quad (\text{S185})$$

and similarly we have,

$$\langle I_{d_2}(t_2) \rangle_{s_2} = e\lambda \mathcal{P}(1 \rightarrow 2), \quad (\text{a constant current in the drain } D_2) \quad (\text{S186})$$

Now, let us generalize the above analysis with stochastic beam of particles from the sources S_1 and S_2 simultaneously. The density matrix in this case is given as follows,

$$\rho_{s_1 s_2} = \sum_{n_1, n_2=0}^{\infty} P_{\lambda}(n_1) P_{\lambda}(n_2) \left[\prod_{i_1=1}^{n_1} \prod_{i_2=1}^{n_2} \tilde{\phi}_{s_2}^{\dagger}(x_2^{(0)}, t_{i_2}^{(0)}) \tilde{\phi}_{s_1}^{\dagger}(x_1^{(0)}, t_{i_1}^{(0)}) | \Omega \rangle \langle \Omega | \tilde{\phi}_{s_1}(x_1^{(0)}, t_{i_1}^{(0)}) \tilde{\phi}_{s_2}(x_2^{(0)}, t_{i_2}^{(0)}) \right], \quad (\text{S187})$$

where the subscript denotes the active sources. Let us focus on the particular case where we have n_1 particles from the source S_1 and n_2 number of particles from the source S_2 . The corresponding quantum state is given as,

$$| \psi_{n_1 n_2} \rangle_{s_1 s_2} = \prod_{i_1=1}^{n_1} \prod_{i_2=1}^{n_2} \tilde{\phi}_{s_2}^{\dagger}(x_2^{(0)}, t_{i_2}^{(0)}) \tilde{\phi}_{s_1}^{\dagger}(x_1^{(0)}, t_{i_1}^{(0)}) | \Omega \rangle. \quad (\text{S188})$$

Let us assume that the detectors, D_1 at x_1 and D_2 at x_2 measures at time t_1 and t_2 . Next, we calculate the density-density correlations at the detector D_1 and D_2 averaged over the emission times $\{t_{i_1}^{(0)}, t_{i_2}^{(0)}\}$. We also assume that the time interval over which we average (T) is large, this implies,

$$\frac{v^2}{T^{n_1} T^{n_2}} \int_{-T/2}^{T/2} \prod_{i_1=1}^{n_1} dt_{i_1} \prod_{i_2=1}^{n_2} dt_{i_2} \langle n_{d_1}(t_1) n_{d_2}(t_2) \rangle_{n_1 n_2} = \frac{v^2}{T^{n_1} T^{n_2}} \int_{-T/2}^{T/2} \prod_{i_1=1}^{n_1} dt_{i_1} \prod_{i_2=1}^{n_2} dt_{i_2} \langle \psi_{n_1 n_2} | n_{d_1}(t_1) n_{d_1}(t_2) | \psi_{n_1 n_2} \rangle, \quad (\text{S189})$$

$$= \frac{n_1 n_2}{T^2} P(11)_{\text{CW}} \mp \frac{2n_1 n_2}{T^2} \mathcal{F}(x_1, t_1; x_2, t_2) \quad (\text{S190})$$

$$+ \frac{2}{T^2} \binom{n_1}{2} P(20)_{\text{CW}} \pm \frac{2}{T^2} \binom{n_1}{2} \mathcal{F}(x_1, t_1; x_2, t_2) \quad (\text{S191})$$

$$+ \frac{2}{T^2} \binom{n_2}{2} P(02)_{\text{CW}} \pm \frac{2}{T^2} \binom{n_2}{2} \mathcal{F}(x_1, t_1; x_2, t_2), \quad (\text{S192})$$

where the subscript outside the angular brackets on LHS emphasizes that we are working with a particular state $| \psi_{n_1 n_2} \rangle_{s_1 s_2}$ and the function \mathcal{F} is given as follows,

$$\mathcal{F}(x_1, t_1; x_2, t_2) = - \left| \int dk_1 e^{ik_1(x_1+x_2+vt_2-vt_1)} \mathcal{T}_{k_1} \mathcal{R}_{k_1}^* | \phi(k_1) |^2 \right|^2. \quad (\text{S193})$$

In obtaining the Eq. (S189), we have assumed that emission is small enough such that as any instant in time there are no more than two particles in the collider. Now, from Eq. (S189) we subtract the contribution when a single source is turned off, this implies we have the following,

$$v^2 \langle n_{d_1}(t_1) n_{d_2}(t_2) \rangle_{n_1 n_2} - v^2 \langle n_{d_1}(t_1) n_{d_2}(t_2) \rangle_{n_1} - v^2 \langle n_{d_1}(t_1) n_{d_2}(t_2) \rangle_{n_2} = \frac{n_1 n_2}{T^2} P(11)_{\text{CW}} \mp \frac{2n_1 n_2}{T^2} \mathcal{F}(x_1, t_1; x_2, t_2). \quad (\text{S194})$$

Averaging over the Poisson distributed particles (n_1 and n_2), we are going to have,

$$v^2 \langle n_{d_1}(t_1) n_{d_2}(t_2) \rangle_{s_1 s_2} - v^2 \langle n_{d_1}(t_1) n_{d_2}(t_2) \rangle_{s_1} - v^2 \langle n_{d_1}(t_1) n_{d_2}(t_2) \rangle_{s_2} = \lambda^2 P(11)_{\text{CW}} \mp 2\lambda^2 \mathcal{F}(x_1, t_1; x_2, t_2), \quad (\text{S195})$$

by writing everything in terms of currents we are going to have,

$$\frac{\langle I_{d_1}(t_1)I_{d_2}(t_2) \rangle_{s_1 s_2}}{\langle I_{s_1} \rangle \cdot \langle I_{s_2} \rangle} - \frac{\langle I_{d_1}(t_1)I_{d_2}(t_2) \rangle_{s_1}}{\langle I_{s_1} \rangle \cdot \langle I_{s_1} \rangle} - \frac{\langle I_{d_1}(t_1)I_{d_2}(t_2) \rangle_{s_2}}{\langle I_{s_2} \rangle \cdot \langle I_{s_2} \rangle} = P(11)_{\text{CW}} - 2\mathcal{F}(x_1, t_1; x_2, t_2), \quad (\text{S196})$$

where we have defined the following,

$$\langle I_{s_1} \rangle = e\lambda = \langle I_{s_2} \rangle \quad (\text{average constant current at the sources } S_1 \text{ and } S_2). \quad (\text{S197})$$

Since our detectors are equidistant from the collider but on the opposite side, Fig. 1a, we have have, $x_1 + x_2 = 0$. Now consider the equal time cross-current correlator, we obtain the Eq. (5) of the main text,

$$\frac{\langle I_{d_1}(t_1)I_{d_2}(t_1) \rangle_{s_1 s_2}}{\langle I_{s_1} \rangle \cdot \langle I_{s_2} \rangle} - \frac{\langle I_{d_1}(t_1)I_{d_2}(t_1) \rangle_{s_1}}{\langle I_{s_1} \rangle \cdot \langle I_{s_1} \rangle} - \frac{\langle I_{d_1}(t_1)I_{d_2}(t_1) \rangle_{s_2}}{\langle I_{s_2} \rangle \cdot \langle I_{s_2} \rangle} = P(11)_{\text{CW}} - 2\mathcal{F}(0) = P(11)_{\text{F}}, \quad (\text{S198})$$

where the antibunching probability, $P(11)_{\text{F}}$ is as shown in Fig. 2a,b and also obtained previously in Sec. II. For extracting the true mutual statistics we would like to write down the benchmark \mathcal{B}_2 , Eq. (S147) in terms of currents and using Eq.(S185)-(S186) we get,

$$\mathcal{B}_2 = \frac{\langle I_{d_1}(t_1) \rangle_{s_1}}{\langle I_{s_1} \rangle} \frac{\langle I_{d_2}(t_2) \rangle_{s_2}}{\langle I_{s_2} \rangle} + \frac{\langle I_{d_1}(t_1) \rangle_{s_2}}{\langle I_{s_2} \rangle} \frac{\langle I_{d_2}(t_2) \rangle_{s_1}}{\langle I_{s_1} \rangle} = P(11)_{\text{CW}}. \quad (\text{S199})$$

Now consider the following with the benchmark,

$$P(11)_{\text{F}} - \mathcal{B}_2 = P(11)_{\text{F}} - P(11)_{\text{CW}} \quad (\text{S200})$$

$$= \frac{\langle I_{d_1}(t_1)I_{d_2}(t_2) \rangle_{s_1 s_2}}{\langle I_{s_1} \rangle \cdot \langle I_{s_2} \rangle} - \frac{\langle I_{d_1}(t_1)I_{d_2}(t_2) \rangle_{s_1}}{\langle I_{s_1} \rangle \cdot \langle I_{s_1} \rangle} - \frac{\langle I_{d_1}(t_1)I_{d_2}(t_2) \rangle_{s_2}}{\langle I_{s_2} \rangle \cdot \langle I_{s_2} \rangle}, \quad (\text{S201})$$

$$- \frac{\langle I_{d_1}(t_1) \rangle_{s_1}}{\langle I_{s_1} \rangle} \frac{\langle I_{d_2}(t_2) \rangle_{s_2}}{\langle I_{s_2} \rangle} - \frac{\langle I_{d_1}(t_1) \rangle_{s_2}}{\langle I_{s_2} \rangle} \frac{\langle I_{d_2}(t_2) \rangle_{s_1}}{\langle I_{s_1} \rangle}, \quad (\text{S202})$$

$$= -2\mathcal{F}(x_1, t_1; x_2, t_2). \quad (\text{S203})$$

The above is simply a function of $t = t_1 - t_2$ and zero-frequency Fourier transform of this leads to the following,

$$\int_{-T/2}^{T/2} dt \left[\frac{\langle I_{d_1}(t_1)I_{d_2}(t_2) \rangle_{s_1 s_2}}{\langle I_{s_1} \rangle \langle I_{s_2} \rangle} - \frac{\langle I_{d_1}(t_1)I_{d_2}(t_2) \rangle_{s_1}}{\langle I_{s_1} \rangle \langle I_{s_1} \rangle} - \frac{\langle I_{d_1}(t_1)I_{d_2}(t_2) \rangle_{s_2}}{\langle I_{s_2} \rangle \langle I_{s_2} \rangle} \right] \quad (\text{S204})$$

$$- \frac{\langle I_{d_1}(t_1) \rangle_{s_1}}{\langle I_{s_1} \rangle} \frac{\langle I_{d_2}(t_2) \rangle_{s_2}}{\langle I_{s_2} \rangle} - \frac{\langle I_{d_1}(t_1) \rangle_{s_2}}{\langle I_{s_2} \rangle} \frac{\langle I_{d_2}(t_2) \rangle_{s_1}}{\langle I_{s_1} \rangle} \Big] = -2 \int_{-T/2}^{T/2} dt \mathcal{F}(x_1, t_1; x_2, t_2). \quad (\text{S205})$$

This can be evaluated as (assuming T is very large),

$$-2 \int_{-T/2}^{T/2} dt \mathcal{F}(x_1, t_1; x_2, t_2) = 2 \int_{-T/2}^{T/2} dt \left[\int dk_1 e^{ik_1(x_1+x_2+vt_2-vt_1)} \mathcal{T}_{k_1} \mathcal{R}_{k_1}^* |\phi(k_1)|^2 \right] \quad (\text{S206})$$

$$\times \int dk_2 e^{-ik_2(x_1+x_2+vt_2-vt_1)} \mathcal{T}_{k_2}^* \mathcal{R}_{k_2} |\phi(k_2)|^2 \Big], \quad (\text{S207})$$

$$= 2 \left[\int dk_1 e^{ik_1(x_1+x_2)} \mathcal{T}_{k_1} \mathcal{R}_{k_1}^* |\phi(k_1)|^2 \right] \quad (\text{S208})$$

$$\times \int dk_2 e^{-ik_2(x_1+x_2)} \mathcal{T}_{k_2}^* \mathcal{R}_{k_2} \int_{-T/2}^{T/2} dt e^{iv(t_2-t_1)[k_1-k_2]}, \quad (\text{S209})$$

$$= \frac{4\pi}{v} \left[\int dk_2 dk_1 e^{ik_1(x_1+x_2)} \mathcal{T}_{k_1} \mathcal{R}_{k_1}^* |\phi(k_1)|^2 \right] \quad (\text{S210})$$

$$\times e^{-ik_2(x_1+x_2)} \mathcal{T}_{k_2}^* \mathcal{R}_{k_2} |\phi(k_2)|^2 \delta(k_1 - k_2) \Big], \quad (\text{S211})$$

$$= \frac{4\pi}{v} \int dk |\mathcal{T}_k|^2 |\mathcal{R}_k|^2 |\phi(k)|^4. \quad (\text{S212})$$

This implies that the zero-frequency Fourier transform is positive definite of fermions and a similar analysis gives a negative definite value of bosons.

VIII. $g^{(2)}(t_1, t_2)$ -FUNCTION AND ITS RELATION TO TIME-RESOLVED CURRENT AUTO-CORRELATOR

In this section we are going to calculate the density-density correlations at a given detector, say, D_1 measured at different times t_1 and t_2 . In the literature, this is known as the $g^{(2)}$ -function [45]. In the subsection VIII A, we perform a pedagogical exercise, where we have just two incoming particles from each of the sources, S_1 and S_2 and denote the density-density correlator in this case with $g^{(2)}$. In the following subsection VIII B, we generalize the formalism for a stochastic beam of particles from the sources. We perform an averaging for a dilute stochastic beam of particles over the emission times and denote the density-density correlator in this case with $\bar{g}^{(2)}$. We demonstrate how, one can extract the mutual statistics of the colliding particles by studying the zero-frequency Fourier transform of the irreducible part of $\bar{g}^{(2)}$. Also, we demonstrate how the time resolved $\bar{g}^{(2)}$ -function can be used to detect the non-point-like geometry of the colliders.

A. $g^{(2)}(t_1, t_2)$ -function for two incoming particles (a pedagogical introduction)

Consider, an incoming state with two particles, one from each source. The $g^{(2)}$ -function is defined as follows,

$$g^{(2)}(t_1, t_2) = v^2 \langle \psi | n_{d_1}(t_1) n_{d_1}(t_2) | \psi \rangle, \quad (\text{S213})$$

where the expectation value is calculated with respect to the following incoming state,

$$|\psi\rangle = \tilde{\phi}_{s_1}^\dagger(x_1^{(0)}, t_1^{(0)}) \tilde{\phi}_{s_2}^\dagger(x_2^{(0)}, t_2^{(0)}) |\Omega\rangle. \quad (\text{S214})$$

From here one can write down the $g^{(2)}(t_1, t_2)$ as follows [27],

$$g^{(2)}(t_1, t_2) = v^2 |\langle \Omega | \phi(x_1, t_1) \phi(x_1, t_2) \tilde{\phi}_{s_1}^\dagger(x_1^{(0)}, t_1^{(0)}) \tilde{\phi}_{s_2}^\dagger(x_2^{(0)}, t_2^{(0)}) | \Omega \rangle|^2. \quad (\text{S215})$$

This implies,

$$g^{(2)}(t_1, t_2) = v^2 |\mathcal{I}_1(x_1, t_1; x_1^{(0)}, t_1^{(0)}) \mathcal{J}_2(x_1, t_2; x_2^{(0)}, t_2^{(0)}) \pm \mathcal{I}_1(x_1, t_2; x_1^{(0)}, t_1^{(0)}) \mathcal{J}_2(x_1, t_1; x_2^{(0)}, t_2^{(0)})|^2, \quad (\text{S216})$$

where the signs $+/-$ correspond to bosons/fermions and the expressions for \mathcal{I}_1 and \mathcal{J}_2 appear in the two-particle amplitudes in Eqs. (S46) and (S48). The function $g^{(2)}(t_1, t_2)$, Eq. (S216), is plotted in Fig. S2c-d under the assumption that the tunneling points to the QAD from the chiral edge states, Fig. 1a, are at equal distances from the sources and the emission happens at the same time, $t_1^{(0)} = t_2^{(0)}$. Now, let us try to understand the behavior of the $g^{(2)}(t_1, t_2)$ in the

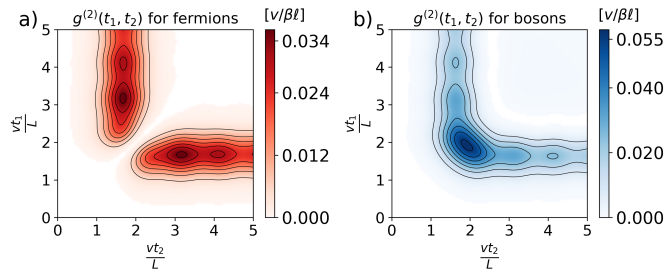


Figure S2. The pair-correlation function $g^{(2)}(t_1, t_2)$ [see Eq. (S216)] for fermions/bosons that arrive simultaneously at the collider but are detected at times t_1, t_2 in the same drain. The wave packets are emitted simultaneously at $t = 0$ and the collider is at a distance $5L/6$ from the sources and the detectors. We use $\frac{\ell}{L} = 2.5$, $k_f = 0$, $r = 0.95$, $\theta = 0$ and a finite temperature $\beta^{-1} = eV/75$, see Sec. IV A of SM [47]. (a) *Fermions*. The function $g^{(2)}$ is generally non-vanishing in an extended collider (hence a characteristic feature), unlike in the case of a point-like collider. Vanishing of $g^{(2)}$ at $t_1 = t_2$ validates exclusion property of fermions. (b) *Bosons*. Non-vanishing along $t_1 = t_2$ shows that bosons can be found in the same location at the same time.

case where the emission time of the particles are different i.e. $t_1^{(0)} \neq t_2^{(0)}$. Due to the finite width of the wave packets, interference between the wave packets depends on the emission times of the wave packets. If the wave packets are

emitted at very different times, in that case there will no interference in the system and the result will be statistics independent. Consider the following expression for the $g^{(2)}$ -function obtained by expanding Eq. (S216),

$$g^{(2)}(t_1, t_2) = v^2 |\mathcal{I}_1(x_1, t_1; x_1^{(0)}, t_1^{(0)})|^2 |\mathcal{J}_2(x_1, t_2; x_2^{(0)}, t_2^{(0)})|^2 + v^2 |\mathcal{I}_1(x_1, t_2; x_1^{(0)}, t_1^{(0)})|^2 |\mathcal{J}_2(x_1, t_1; x_2^{(0)}, t_2^{(0)})|^2, \quad (\text{S217})$$

$$\pm 2v^2 \text{Re}[\mathcal{I}_1^*(x_1, t_1; x_1^{(0)}, t_1^{(0)}) \mathcal{J}_2^*(x_1, t_2; x_2^{(0)}, t_2^{(0)}) \mathcal{I}_1(x_1, t_2; x_1^{(0)}, t_1^{(0)}) \mathcal{J}_2(x_1, t_1; x_2^{(0)}, t_2^{(0)})], \quad (\text{S218})$$

$$\approx v^2 |\mathcal{I}_1(x_1, t_1; x_1^{(0)}, t_1^{(0)})|^2 |\mathcal{J}_2(x_1, t_2; x_2^{(0)}, t_2^{(0)})|^2 + v^2 |\mathcal{I}_1(x_1, t_2; x_1^{(0)}, t_1^{(0)})|^2 |\mathcal{J}_2(x_1, t_1; x_2^{(0)}, t_2^{(0)})|^2, \quad (\text{S219})$$

where we have used the fact that in the case when the emission time of the wave packets are very different then $\mathcal{I}_1^*(x_1, t_1; x_1^{(0)}, t_1^{(0)}) \mathcal{J}_2(x_1, t_1; x_2^{(0)}, t_2^{(0)}) \rightarrow 0$, because of the finite width of the incoming wave packets. For fermions, in a point-like collider we find that $g^{(2)}(t_1, t_2) = 0$ for all t_1, t_2 , meaning that the two fermions always end up in different drains, $P(11)_F = 1$. In the extended collider generically $g^{(2)}(t_1, t_2) \neq 0$ except for simultaneous detection $t_1 = t_2$, since the two fermions cannot occupy the same position simultaneously in the same detector. By integrating Eq. (S216), we obtain the bunching probability,

$$\frac{1}{2} \iint_{-\infty}^{\infty} dt_1 dt_2 g^{(2)}(t_1, t_2) = P(20)_F, \quad (\text{S220})$$

which is in general non-zero in an extended collider. In order to extract the mutual statistics from the $g^{(2)}$ -function, one can look at the following,

$$g_{\text{Irr}}^{(2)}(t_1, t_2) = v^2 \langle n_{d_1}(t_1) n_{d_1}(t_2) \rangle_{s_1 s_2} - v^2 \langle n_{d_1}(t_1) \rangle_{s_1} \langle n_{d_1}(t_2) \rangle_{s_2} - v^2 \langle n_{d_1}(t_2) \rangle_{s_1} \langle n_{d_1}(t_1) \rangle_{s_2}, \quad (\text{S221})$$

where the subscript refers to the active source(s). This effectively gets rid-off all the single particle self-interference terms and we obtain only statistics dependent part,

$$g_{\text{Irr}}^{(2)}(t_1, t_2) = \pm 2v^2 \text{Re}[\mathcal{I}_1^*(x_1, t_1; x_1^{(0)}, t_1^{(0)}) \mathcal{J}_2^*(x_1, t_2; x_2^{(0)}, t_2^{(0)}) \mathcal{I}_1(x_1, t_2; x_1^{(0)}, t_1^{(0)}) \mathcal{J}_2(x_1, t_1; x_2^{(0)}, t_2^{(0)})], \quad (\text{S222})$$

where the $+/-$ signs are for bosons and fermions. However, if the particles are arriving at the collider at very different times then, there will be less interference between the wave packets and therefore $g_{\text{Irr}}^{(2)}(t_1, t_2) \rightarrow 0$. This result can intuitively be understood from the fact that less interference implies less likely for the particles to wind around each other (exchange processes) and less effect of mutual statistics on the $g_{\text{Irr}}^{(2)}$ -function ($|g_{\text{Irr}}^{(2)}| \ll 1$), Fig. S3. The above presentation assumes that we have two incoming particles from the two different sources, S_1 and S_2 .

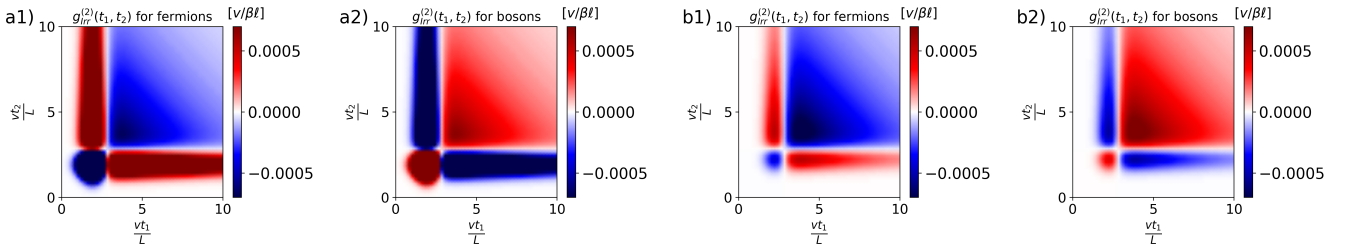


Figure S3. Plot for $g_{\text{Irr}}^{(2)}$ -function for a pair of incoming particles from the sources S_1 and S_2 . (a) $g_{\text{Irr}}^{(2)}$ -function for a pair of (a1) fermions and (a2) bosons without a delay in the arrival times. (b) $g_{\text{Irr}}^{(2)}$ -function for a pair of (b1) fermions and (b2) bosons with a delay L/v in the arrival times.

B. $\bar{g}^{(2)}(t_1, t_2)$ -function for a stochastic beam of particles

In this subsection we are going to generalize the above calculation for a stochastic beam of particles. In one-dimensional channel, current at the detectors is proportional to the number density and is given as, $I_{d_i}(t_i) = evn_{d_i}(t_i)$ where e is electronic charge and v is the velocity and $i = 1, 2$. This implies that the $\bar{g}^{(2)}(t_1, t_2)$ function is an auto-correlator of the currents at a given detector averaged over emission times of the stochastic beam of particles from the sources S_1 and S_2 , Eq. (S187) (the $\bar{\cdot}$ refers to this averaging),

$$\bar{g}^{(2)}(t_1, t_2) = \frac{1}{e^2} \langle I_{d_1}(t_1) I_{d_1}(t_2) \rangle. \quad (\text{S223})$$

[Compare to Eq. (S213).] Let us assume that the sources are turned ON for the interval $[-T/2, T/2]$, we assume in the calculations that $T \rightarrow \infty$. Again, we start by looking at a particular case where we have n_1 particles from S_1 and n_2 particles from source S_2 . By averaging over the incoming times $\{t_{i_1}^{(0)}, t_{i_2}^{(0)}\}$ in the interval $[-T/2, T/2]$, we obtain the following,

$$\bar{g}^{(2)}(t_1, t_2)_{n_1 n_2} = \frac{v^2}{T^{n_1} T^{n_2}} \int_{-T/2}^{T/2} \prod_{i_1=1}^{n_1} dt_{i_1}^{(0)} \prod_{i_2=1}^{n_2} dt_{i_2}^{(0)} \left[\langle n_{d_1}(t_1) n_{d_1}(t_2) \rangle_{n_1 n_2} - \langle n_{d_1}(t_1) n_{d_1}(t_2) \rangle_{n_1} - \langle n_{d_1}(t_1) n_{d_1}(t_2) \rangle_{n_2} \right], \quad (\text{S224})$$

$$= \frac{2n_1 n_2 e^2}{T^2} P(20)_{\text{CW}} \pm \frac{2n_1 n_2 e^2}{T^2} F(t_1, t_2), \quad (\text{S225})$$

where $+/-$ corresponds to bosons and fermions and the subscript ‘‘CW’’ refers to the classical waves and the subscript on the LHS tells us that we are working with a particular state, $|\psi_{n_1 n_2}\rangle_{s_1 s_2}$. By subtracting the contribution from the single active source terms, we remove all the possibility where the two particles comes from the same source, a possibility not accounted in the previous sub-sec. VIII A. The function F is found to be only depend on the time-difference $(t_1 - t_2)$ and is given as follows,

$$F(t_1 - t_2) = \text{Re} \left[\int_{-\infty}^{\infty} dk_1 e^{ik_1 v(t_1 - t_2)} |\phi(k_1)|^2 |\mathcal{T}_{k_1}|^2 \int_{-\infty}^{\infty} dk_2 e^{-ik_2 v(t_1 - t_2)} |\phi(k_2)|^2 |\mathcal{R}_{k_2}|^2 \right]. \quad (\text{S226})$$

For a stochastic beam of particles from the sources S_1 and S_2 with emission rate λ , we can take the average over the Poisson distribution of Eq. (S225) and by noting $F(t_1, t_2) = F(t_1 - t_2)$ we get for a stochastic beam of particles from S_1 and S_2 ,

$$\bar{g}^{(2)}(t_1 - t_2) = 2\lambda^2 P(20)_{\text{CW}} \pm 2\lambda^2 F(t_1 - t_2), \quad (\text{S227})$$

this can further be written as,

$$\frac{1}{2\lambda^2} \bar{g}^{(2)}(t_1 - t_2) = P(20)_{\text{CW}} \pm F(t_1 - t_2). \quad (\text{S228})$$

For extracting the statistics we can define an irreducible $\bar{g}_{\text{Irr}}^{(2)}$ -function by removing the self-interference terms from Eq. (S227) and this is analogous to the action of subtracting the benchmark, \mathcal{B}_2 from $P(11)_{\text{F}}$ as done in section, Sec. V. For a particular state $|\psi_{n_1 n_2}\rangle_{s_1 s_2}$, the irreducible $\bar{g}_{\text{Irr}}^{(2)}(t_1 - t_2)_{n_1 n_2}$ is given as,

$$\bar{g}_{\text{Irr}}^{(2)}(t_1 - t_2)_{n_1 n_2} = \frac{v^2}{T^{n_1} T^{n_2}} \int_{-T/2}^{T/2} \prod_{i_1=1}^{n_1} dt_{i_1} \prod_{i_2=1}^{n_2} dt_{i_2} \left[\langle n_{d_1}(t_1) n_{d_1}(t_2) \rangle_{n_1 n_2} - \langle n_{d_1}(t_1) n_{d_1}(t_2) \rangle_{n_1} - \langle n_{d_1}(t_1) n_{d_1}(t_2) \rangle_{n_2} \right. \quad (\text{S229})$$

$$\left. - \langle n_{d_1}(t_1) \rangle_{n_1} \langle n_{d_1}(t_2) \rangle_{n_1} - \langle n_{d_1}(t_1) \rangle_{n_2} \langle n_{d_1}(t_2) \rangle_{n_2} \right]. \quad (\text{S230})$$

In this case, the reducible terms (that includes self interference terms) can be written as follows,

$$\frac{v^2}{T^{n_1} T^{n_2}} \int_{-T/2}^{T/2} \prod_{i_1=1}^{n_1} dt_{i_1} \prod_{i_2=1}^{n_2} dt_{i_2} \left[\langle n_{d_1}(t_1) \rangle_{s_1} \langle n_{d_1}(t_2) \rangle_{s_1} + \langle n_{d_1}(t_1) \rangle_{s_2} \langle n_{d_1}(t_2) \rangle_{s_2} \right] = \frac{2n_1 n_2}{T^2} \mathcal{P}(1 \rightarrow 1) \mathcal{P}(2 \rightarrow 1), \quad (\text{S231})$$

Taking an average over n_1 and n_2 , leads to $2\lambda^2 \mathcal{P}(1 \rightarrow 1) \mathcal{P}(2 \rightarrow 1) = 2\lambda^2 P(20)_{\text{CW}}$. Hence, for a stochastic beam of particles, we are going to have the following

$$\frac{1}{2\lambda^2} \bar{g}_{\text{Irr}}^{(2)}(t_1 - t_2) = \pm F(t_1 - t_2). \quad (\text{S232})$$

where $+/-$ is for bosons and fermions and it is shown in the Fig. 2c-d. Zero-frequency Fourier transformation (integration over the time difference $t = t_1 - t_2$) of the $\bar{g}_{\text{Irr}}^{(2)}$ -function leads to the following,

$$\frac{1}{2\lambda^2} \int_{-\infty}^{\infty} dt \bar{g}_{\text{Irr}}^{(2)}(t) = \pm \int_{-\infty}^{\infty} dt F(t) = \pm \frac{2\pi}{v} \int_{-\infty}^{\infty} dk |\mathcal{T}_k|^2 |\mathcal{R}_k|^2 |\phi(k)|^4, \quad (\text{S233})$$

which implies that the zero-frequency Fourier transform of irreducible part of the $\bar{g}^{(2)}$ -function is sign definite for bosons (positive) and fermions (negative) and hence determines the statistics. Though the zero-frequency Fourier transform of $\bar{g}_{\text{irr}}^{(2)}$ is sign definite, this is not the case with the $\bar{g}_{\text{irr}}^{(2)}(t)$ function, Eq. (S232). As we vary time, t , the sign changes for both bosons and fermions, see Fig. 2c-d. This is an intrinsic property of an extended collider and is not the case with the point-like collider. In the case of point-like collider, the transmission/reflection coefficients are independent of momentum i.e. $\mathcal{T}_k = \mathcal{T}$ and $\mathcal{R}_k = \mathcal{R}$. As a result of this the $\bar{g}_{\text{irr}}^{(2)}$ which is proportional to F is given as,

$$\frac{1}{2\lambda^2}\bar{g}_{\text{irr}}^{(2)}(t_1 - t_2) = \pm F(t_1 - t_2) = \pm \text{Re} \left[\int_{-\infty}^{\infty} dk_1 e^{ik_1 v(t_1 - t_2)} |\phi(k_1)|^2 |\mathcal{T}_{k_1}|^2 \int_{-\infty}^{\infty} dk_2 e^{-ik_2 v(t_1 - t_2)} |\phi(k_2)|^2 |\mathcal{R}_{k_2}|^2 \right], \quad (\text{S234})$$

$$= \pm \mathcal{T}^2 |\mathcal{R}|^2 \text{Re} \left[\int_{-\infty}^{\infty} dk_1 e^{ik_1 v(t_1 - t_2)} |\phi(k_1)|^2 \int_{-\infty}^{\infty} dk_2 e^{-ik_2 v(t_1 - t_2)} |\phi(k_2)|^2 \right], \quad (\text{S235})$$

$$= \pm |\mathcal{T}|^2 |\mathcal{R}|^2 \left| \int_{-\infty}^{\infty} dk_1 e^{ik_1 v(t_1 - t_2)} |\phi(k_1)|^2 \right|^2, \quad (\text{S236})$$

where $+/-$ is for bosons/fermions. Note that the quantity,

$$|\mathcal{T}|^2 |\mathcal{R}|^2 \left| \int_{-\infty}^{\infty} dk_1 e^{ik_1 v(t_1 - t_2)} |\phi(k_1)|^2 \right|^2 \geq 0, \quad (\text{S237})$$

and does not change sign as we vary $t = t_1 - t_2$. Hence, the sign change in $\bar{g}_{\text{irr}}^{(2)}$, Eq. (S232) for bosons and fermions, Fig. 2c-d is a feature that is restricted to an extended collider.